Molecular Phylogenetics and Evolution 130 (2019) 380–396

Contents lists available at ScienceDirect

Molecular Phylogenetics and Evolution

journal homepage: www.elsevier.com/locate/ympev

The effect of Hengduan Mountains Region (HMR) uplift to environmental changes in the HMR and its eastern adjacent area: Tracing the evolutionary history of *Allium* section *Sikkimensia* (Amaryllidaceae)

Chuan Xie[a], Deng-feng Xie[a], Yan Zhong[a], Xian-Lin Guo[a], Qing Liu[b], Song-Dong Zhou[a], Xing-Jin He[a,*]

[a] Key Laboratory of Bio-Resource and Eco-Environment of Ministry of Education, College of Life Sciences, Sichuan University, Chengdu 610065, Sichuan, PR China
[b] Key Laboratory of Mountain Ecological Restoration and Bioresource Utilization, Chengdu Institute of Biology, Chinese Academy of Sciences, Chengdu 610041, Sichuan, PR China

ARTICLE INFO

Keywords:
Allium section *Sikkimensia*
Hengduan Mountains Region
Qinling-Daba Mountains
Environmental changes
Morphological differences
Species distribution modeling

ABSTRACT

Exploring the effects of orographic events and climatic shifts on geographic distribution of organism in the Hengduan Mountains Region (HMR) and its eastern adjacent area is crucial to the understanding of the environmental changes to organismal evolution. To gain further insight into these processes, we reconstruct evolutionary history of ten species in *Allium* section *Sikkimensia*, distributed across regions abovementioned. Using chloroplast and nuclear sequence variation of 79 populations of these ten *Allium* species with known morphological preferences, we elucidate the phylogenetic relationship, divergence time, ancestral area and genetic structures. Climatic variables analysis, Isolation by distance (IBD) and environment (IBE) and Species distribution modeling (SDM) were analyzed along different genetic clades. These analyses indicated that the initial split of *Sikkimensia* was triggered by climate changes following Qinghai-Tibet Plateau *sensu lato* (QTP*sl*) uplift during the late Miocene. Subsequently, divergences within lineage (lineage A)/among lineages (lineage C and D) in *Sikkimensia* may be induced by the intense uplift of the HMR around 3–4 Ma and abrupt intensifying of the Asian monsoon regimes. Furthermore, *Sikkimensia* populations exhibited lopsided demographic history in the Last Glacial Maximum (LGM), as was indicated by the expansion of their range in the QDM and contraction in the HMR. Our findings appear to suggest that the HMR uplift could have strengthened the orographic difference between the HMR and its eastern adjacent area and led to a colder climate in the HMR, while geological topography also played an important role for taxa to respond the climate change that had taken place in the HMR and its eastern adjacent area during the Pleistocene.

1. Introduction

Geological events and climatic shifts are widely acknowledged to have profoundly shaped the organismal evolution (Antonelli et al., 2009; Wen et al., 2014; Favre et al., 2015; Li et al., 2016). The Hengduan Mountains Region (HMR) is the southeastern section of the Qinghai-Tibet Plateau *sensu lato* (QTP*sl*, including the Qinghai-Tibet Plateau *sensu stricto* (QTP*ss*), Himalayas, Hengduan Mountains) (Zhang et al., 2002; Liang et al., 2018), and it is a key reservoir of global biodiversity hotspot (Myers et al., 2000; Marchese, 2015). This region was formed by the India-Eurasia collision during the Cenozoic, and the consequent rise of the QTP*sl* (Yin and Harrison, 2000; Rowley and Currie, 2006; Royden et al., 2008; Lippert et al., 2014). However, the exact scale and timing of the QTP*sl* uplift is a longstanding controversy (Harrison et al., 1992; Li and Fang, 1999; Royden et al., 2008; Lippert et al., 2014; Favre et al., 2015; Renner, 2016; Ding et al., 2017). Yet, one thing is for sure, that is, as the southeastern section of the highest and largest plateau in the world, the formation and development of the HMR deeply affects evolution of ecological system in western China and neighboring areas (Shi et al., 1995; Zheng, 1996). In spite of the fact that quantifying the response of organisms to the orogenic process has been considered a huge challenge, elucidating the evolutionary history and adaptation of plant in this region are of great interest (Liu et al., 2014; Wen et al., 2014).

The uplift of the QTP*sl* not only had created the spectacular plateau landform on the earth, but also had caused large scale changes in

* Corresponding author.
E-mail address: xjhe@scu.edu.cn (X.-J. He).

https://doi.org/10.1016/j.ympev.2018.09.011
Received 26 March 2018; Received in revised form 29 August 2018; Accepted 17 September 2018
Available online 18 September 2018
1055-7903/

climatic region, river system and distribution of vegetation, which in turn profoundly affected the biological processes in the QTP*sl* and adjacent regions (Li and Fang, 1999). An increasing number of paleoclimatic and paleogeological evidence, in conjunction with simulated modeling studies, has supported that the QTP*sl* uprising played a critical role to the East Asian climate changes (An et al., 2001; Guo et al., 2002; Liu and Dong, 2013). The Himalayas and the neighboring mountains as barriers obstructing the Indian and Pacific Ocean monsoons, have dominantly strengthened the QTP*ss* (a term that refers only to the platform; Xing and Ree, 2017) aridification (Boos and Kuang, 2010, 2013). Simultaneously, the East Himalaya region has a humid and warm climate as a result of uplift of the QTP*sl* (An et al., 2001; Wan et al., 2007; Chang et al., 2010). The Miocene cooling coincident with the Cenozoic uplift of the plateau is supported by the geological records of the QTP*ss* (George et al., 2001). These orogenic and environmental changes, resulting from the uplift, have likely served as a major force in speciation, origin of the lineage and plant evolution throughout the QTP*sl* and adjacent region (Farve et al., 2015; Zhao et al., 2015; Meng et al., 2017). However, most of these previous studies have always focused on the response patterns of plant to orogenic and climatic changes, involving the QTP*ss*, Himalayas and Hengduan Mountains (Opgenoorth et al., 2010; Xu et al., 2010; Liu et al., 2013; Li et al., 2016; Luo et al., 2016; Meng et al., 2017), whereas little is known about the effects of the orogenic and climate events on herbal species throughout the HMR and its eastern adjacent area (Qinling-Daba Mountians, QDM).

The Quaternary climatic fluctuations likewise had profound effect on population distribution and demographic history of plant in Northern Hemisphere, causing range shifts or extinction, as well as possibly driving local adaptation (Davis and Shaw, 2001; Hewitt, 2004; Hickerson et al., 2010). Repeated glacial retreats and postglacial expansions was a main model for many plants in Northern Hemisphere to undergo the Quaternary (Hewitt, 1996, 1999). In the QTP*sl* and adjacent region, periglacial zone located in the low altitude area of the southeastern of the QTP*sl* was crucial glacial refugia for endemic species *in situ* (Qiu et al., 2011; Gao et al., 2012; Liu et al., 2014). In addition, many studies suggested that species may have survived at high altitude area in the QTP*sl* during the Quaternary glacial cycle (Opgenoorth et al., 2010; Liu et al., 2012; Luo et al., 2016; Meng et al., 2017). Previous studies have mainly focused on the effects of the Quaternary climatic oscillations in the QTP*sl*, especially in the HMR and adjacent region on the species-level diversification and the demography of populations (Zhang et al., 2005; Yang et al., 2008, 2012; Xu et al., 2010; Jia et al., 2011; Luo et al., 2016; Shahzad et al., 2017). However, few studies have been reported, involving the response of the plant distributed in the QTP*sl* and out of the QTP*sl* to Pleistocene climate changes. Accordingly, we expect the distribution and demographic history of the plant taxa distributed across the HMR and the QDM to display demographic responses to the Pleistocene climate changes.

Section *Sikkimensia* (Traub) N. Friesen of *Allium* L occurs manly in Central-southwest China (Fritsch, 2001; Fritsch and Frieren, 2002; Friesen et al., 2006; Li et al., 2010). The recent phylogenetic study indicated that this section forms a distinct monophyletic clade and comprises two groups (Li et al., 2010). According to records of section *Sikkimensia* in the *Flora of China*, thirteen morphologically distinct species are distributed in the QTP*sl* and adjacent regions with altitudinal ranges from 1400 m to 5000 m. There are some interesting phenomenon: six species with purple-blue flower and filament and stigma within perianth pale are largely distributed in the HMR (*A. forrestii* Diels, *A. changduense* J. M. Xu in F. T. Wang & Tang, *A. sikkimense* Baker, *A. beesianum* W. W. Smith and *A. yuanum* F. T. Wang & Tang, except *A. plurifoliatum* var. *zhegushanense* J. M. Xu in F. T. Wang & Tang with filament and stigma outside perianth pale); two species with pink-white flower and filament and stigma outside perianth pale are distributed in the QDM and adjacent region (including *A. plurifoliatum* var. *plurifoliatum* Rendle and *A. paepalanthoides* Airy Shaw); five species are distributed across the HMR, the QDM and adjacent region with purple-blue flower and filament and stigma outside perianth pale (contains *A. cyaneum* Regel, *A. stenodon* Nakai &Kitagawa, *A. henryi* C. H. Wright, *A. heteronema* F. T. Wang & Tang and *A. aciphyllum* J. M. Xu in F. T. Wang & Tang). Because of the distinctive distribution patterns (span the the QTP*sl* and the QDM and adjacent region) and significant morphological clustering (Fig. S1), the evolutionary processes of the section *Sikkimensia* may to provide insight into underlying environmental changes caused by uplift of the Hengduan Mountains and Quaternary ice cycles.

In this study, our attention was focused on ten species in the section *Sikkimensia*. We tested for correspondence between genetic structure, morphological variation and climatic differences and used a phylogeographic approach to elucidate the mechanism of the divergence and population evolutionary history in the section *Sikkimensia*. Our aims are: (1) to identify the phylogenetic relationships within the section *Sikkimensia* on population level; (2) to explore the effects of geological and climate changes to the geographic distribution of plant throughout the HMR and its eastern adjacent area; (3) to compare the contributions of Pleistocene glacial cycles to changes in distribution shift and genetic diversity of plant throughout the HMR and its eastern adjacent area.

2. Materials and methods

2.1. Plant sampling

In 2012 to 2016, 718 individuals belonged to ten species of *Allium* section *Sikkimensia* from 79 natural populations were collected in this study (see Table 1). *Allium aciphyllum* have not been collected (because the only recorded location had been destroyed by tunnel project). Two species from *Allium* section *Sikkimensia*, i.e., *A. forrestii* and *A. changduense*, as well as *A. rude* and *A. chrysocephalum* were chosen as outgroups based on previous study (Freisen et al., 2006; Li et al., 2010). To avoid collecting the same genetype, the distance between the sampled individuals was at least 10 m. Fresh leaves of representative individuals were collected from each population and dried in silica gel. The voucher specimens were deposited in Sichuan University Herbarium (SZ).

In this study, we examined thirteen morphological characteristics for every individual from each population: nine flower traits, three leaf traits and one bulb trait (See Table S1), as well as the habitat (Table S2). The mean values of the morphological characteristics of total populations were used to Principal component analysis (PCA).

2.2. DNA extraction, PCR amplification and sequencing

Total genomic DNA was extracted from the dried leaf tissue by a modified cetyltrimethyl ammonium (CTAB) protocol (Doyle and Doyle, 1987). For the polymerase chain reaction (PCR), we selected nrITS (nrITS1-5.8sRNA-nrITS2) (White et al., 1990) and ETS fragment (Wright et al., 2001), as well as five chloroplast fragments (atpI-atpH, petL-psbE, trnC-rpoB, trnV-ndhC, trnL-trnF) (Shaw et al., 2005, 2007). PCRs were performed in a 30 μL volume with 3 μL plant total DNA, 1.5 μL forward primer, 1.5 μL reverse primer and 15 μL volume 2 × Taq MasterMix (cwbio, Beijing, China). The primer sequences and amplification conditions are listed in Table S3. All sequences in this study were sequenced from both directions and were deposited in GenBank with accession numbers MF674579-MF677750 and MH065758-MH067951.

2.3. Phylogeny reconstruction

All the DNA sequences were edited by SeqMan (DNAstar package; DNAStar Inc., Madison, WI, USA) for obtaining consensus sequences. CLUSTAL X version 2.0 (Larkin et al., 2007) was used to align with subsequent manual adjustments. Haplotypes were identified and distinguished using DNAsp version 5.0 (Librado and Rozas, 2009). The phylogeny reconstruction based on haplotype was performed in Bayesian inference (BI), maximum parsimony (MP) and maximum likelihood (ML). The BI analysis was conducted with MrBayes version 3.2

Table 1
Information of sample location and sample size of 79 populations of the ten species within the section *Sikkimensia*, the chloroplast haplotypes (C) and nuclear haplotypes (N).

Population code	Location	Latitude	Longitude	Altitude (m)	Sample	Chloroplast Haplotypes (C)	Nuclear Haplotype (N)
Allium yuanum (yua)							
yua1	Jiuzhaigou, SiChuan	33.3488	103.5564	3600	10	C1(10)	N1(10)
yua2	Songpan, SiChuan	32.6665	103.7274	3700	10	C2(10)	N1(10)
Allium beesianum (bee)							
bee1	Jianchuan, YunNan	26.6524	99.6963	3800	10	C3(10)	N2(10)
bee2	Lijiang, YunNan	27.1862	100.2107	4000	10	C3(11)	N3(10)
Allium sikkimense (sik)							
sik1	Banma, QingHai	32.6745	100.9637	3700	10	C4(6), C5(2), C13(2)	N4(10)
sik2	Basu, XiZang	30.2197	96.6822	3260	6	C3(6)	N5(6)
sik3	Baoxing, SiChuan	30.9937	102.7497	4000	7	C1(7)	N6(7)
sik4	Chengduo, QingHai	33.2585	97.0825	4200	6	C5(6)	N5(1), N7(5)
sik5	Changdu, XiZang	31.7616	97.7646	4303	10	C3(10)	N8(10)
sik6	Cuona, XiZang	27.9853	91.9483	4341	5	C3(5)	N9(5)
sik7	Chayu, XiZang	28.5938	97.9663	3920	10	C6(10)	N5(3), N10(7)
sik8	Daofu, SiChuan	30.8405	101.1547	3434	10	C5(3), C7(7)	N4(2), N5(1), N11(7)
sik9	Deqing, YunNan	28.7901	99.0287	4100	10	C1(2), C8(8)	N5(10)
sik10	Datong, QingHai	36.4444	101.5519	2930	5	C1(5)	N12(5)
sik11	Ganzi, SiChuan	31.3123	99.6097	4094	10	C5(9), C7(1)	N13(10)
sik12	Hongyuan, SiChuan	33.1282	102.6685	3000	10	C9(8), C14(2)	N4(5), N14(5)
sik13	Jiangda, SiChuan	31.8371	98.2404	4251	10	C3(4), C10(6)	N15(10)
sik14	Jiulong, SiChuan	29.1128	101.169	3761	10	C11(10)	N16(8), N21(2)
sik15	Jiuzhi, QingHai	32.9359	100.736	3650	10	C1(10)	N5(3), N17(7)
sik16	Jiuzhaigou, SiChuan	33.3855	103.6097	3500	10	C1(2), C3(6), C9(1), C14(1)	N4(10)
sik17	Luding, SiChuan	29.885	102.0184	3510	10	C12(10)	N6(1), N18(9)
sik18	Luqu, GanSu	34.7004	102.7967	3458	10	C1(10)	N19(10)
sik19	Leiwuqi, XiZang	31.4797	96.3789	4278	10	C3(10)	N8(4), N20(6)
sik20	Langxian, XiZang	28.3757	93.1464	4500	4	C3(4)	N9(4)
sik21	Mangkang, XiZang	29.6987	98.5587	4586	10	C3(10)	N5(10)
sik22	Muli, SiChuan	27.867	101.0567	4100	6	C1(6)	N21(6)
sik23	Maqin, QingHai	34.4225	100.2891	3800	10	C13(10)	N4(2), N22(8)
sik24	Meixian, ShaanXi	33.9754	107.4989	3200	10	C1(10)	N23(10)
sik25	Ruoergai, SiChuan	33.524	103.247	3500	10	C3(3), C14(7)	N4(10)
sik26	Seda, SiChuan	32.2594	100.3109	3916	10	C5(1), C10(2), C15(7)	N4(1), N24(9)
sik27	Songpan, SiChuan	32.3024	103.0743	3100	10	C16(10)	N22(10)
sik28	Suoxian, XiZang	31.7848	93.7497	4113	10	C17(10)	N9(10)
sik29	Wenchuan, SiChuan	30.904	102.3813	4500	10	C18(10)	N25(10)
sik30	Xiangcheng, SiChuan	29.0433	99.7774	4076	10	C3(3), C19(7)	N26(10)
Allium plurifoliatum var. *zhegushanense* (zhe)							
zhe	Zhegushan, SiChuan	32.9032	102.6517	3350	10	C20(10)	N27(10)
Allium cyaneum (cya)							
cya1	Banma, QingHai	32.6745	100.9637	3700	10	C21(10)	N28(10)
cya2	Chengduo, QingHai	33.3233	96.984	4200	5	C22(5)	N29(5)
cya3	Cuona, XiZang	27.9853	91.9483	4370	10	C23(10)	N30(10)
cya4	Daofu, SiChuan	31.2935	101.1879	3184	10	C24(10)	N28(1), N31(9)
cya5	Henan, QingHai	35.3347	101.9494	3400	6	C25(6)	N28(6)
cya6	Jiuzhaigou, SiChuan	33.3855	103.6097	2600	10	C21(1), C24(1), C26(6), C31(2)	N28(2), N32(8)
cya7	Lajia, QingHai	35.6715	100.5437	3100	10	C21(10)	N28(1), N33(9)
cya8	Luqu, GanSu	34.7711	102.8919	3290	10	C27(10)	N34(10)
cya9	Maqin, QingHai	34.4225	100.2891	3800	10	C21(10)	N28(10)
cya10	Meixian, ShaanXi	34.0327	107.8255	2277	10	C28(8), C30(2)	N35(10)
cya11	Ningwu, ShanXi	38.8262	112.2352	2530	10	C29(10)	N36(10)
cya12	Pingliang, GanSu	35.5031	106.247	2000	4	C28(1), C30(3)	N35(4)
cya13	Qumalai, QingHai	33.3995	96.7632	4000	6	C22(6)	N29(6)
cya14	Ruoergai, SiChuan	33.5128	103.2393	3400	10	C31(10)	N28(1), N32(2), N37(7)
cya15	Shennongjia, HuBei	31.4513	110.3231	2700	10	C32(10)	N38(10)
cya16	Songpan, SiChuan	32.8629	103.5448	3100	10	C24(8), C26(2)	N32(3), N39(7)
cya17	Suoxian, XiZang	31.7848	93.7497	4113	10	C33(10)	N40(10)
cya18	Tanchang, GanSu	34.129	104.5118	2300	10	C21(2), C26(1), C34(7)	N41(10)
cya19	Wutaishan, ShanXi	39.3954	113.6697	1992	10	C35(10)	N42(10)
cya20	Xinghai, QingHai	35.3404	100.2591	3400	6	C21(6)	N43(6)
cya21	Yuanqu, ShanXi	35.4091	111.9608	2024	10	C29(10)	N44(10)
cya22	Zhouqu, GanSu	33.5361	104.2474	2700	10	C26(2), C34(8)	N41(10)
cya23	Zhashui, ShaanXi	33.7103	108.3823	2183	10	C29(10)	N45(10)
Allium stenodon (ste)							
ste	Xinglong, HeBei	40.5737	117.3973	2000	10	C36(10)	N48(10)
Allium henryi (hen)							
hen	Shennongjia, HuBei	31.5001	110.1516	2200	6	C37(6)	N47(6)
Allium heteronema (het)							
het	Chengkou, ChongQing	31.5891	108.988	2300	3	C38(3)	N46(3)

(*continued on next page*)

Table 1 (*continued*)

Population code	Location	Latitude	Longitude	Altitude (m)	Sample	Chloroplast Haplotypes (C)	Nuclear Haplotype (N)
Allium plurifoliatum var. *plurifoliatum* (plu)							
plu1	Huayin, shaanxi	34.2952	109.8168	1977	10	C39(10)	N49(10)
plu2	Jiuzhaigou, SiChuan	33.1142	103.8725	2243	10	C40(10)	N50(7), N54(3)
plu3	Meixian, ShaanXi	33.7253	107.6632	2400	10	C41(10)	N51(6), N52(4)
plu4	Pingliang, GanSu	35.297	106.3883	2011	10	C42(10)	N51(2), N52(8)
plu5	Pingwu, SiChuan	32.5679	104.6713	1950	10	C43(5), C44(5)	N50(1), N53(7), N54(2)
plu6	Qingchuan, SiChuan	32.6438	104.7249	2207	10	C43(2), C44(7), C45(1)	N53(5), N54(5)
plu7	Tanchang, GanSu	33.6195	104.3958	2200	10	C44(1), C45(9)	N54(10)
Allium paepalanthoides (pae)							
pae1	Fangshan, ShanXi	37.577	111.3768	1888	10	C46(8), C49(2)	N55(10)
pae2	Huixian, GanSu	33.6593	106.3827	1807	10	C47(5), C48(2), C50(1), C56(2)	N56(8), N57(2)
pae3	Huxian, ShaanXi	33.7875	108.8287	1335	10	C48(7), C50(3)	N57(10)
pae4	Lishi, ShanXi	37.6242	111.0557	1794	10	C46(1), C49(9)	N55(10)
pae5	Ningshan, ShaanXi	33.3917	108.6053	1804	10	C50(10)	N57(10)
pae6	Puxian, ShanXi	36.5527	111.1777	1550	10	C51(10)	N55(10)
pae7	Shennongjia, HuBei	31.4596	110.2444	1570	10	C52(10)	N58(10)
pae8	Songxian, HeNan	34.1359	111.4876	1050	8	C53(8)	N59(8)
pae9	Yongji, ShanXi	34.8097	110.5076	1353	10	C54(10)	N60(10)
pae10	Yuanqu, ShanXi	35.5074	111.8962	1874	5	C55(5)	N55(5)
pae11	Zhouzhi, ShaanXi	33.6543	107.8541	1672	10	C50(5), C56(5)	N57(3), N61(7)
Total 79					718		

(Ronquist et al., 2012). MrModelTest 2.2 was used to select a best-model of nucleotide substitution, and the HKY + G and GTR + I + G model under the Akaike information criterion (AIC) were selected in nrDNA and cpDNA, respectively. The Bayesian Markov chain Monte Carlo (MCMC) searches was performed for 2×10^7 generations with four chains and sampling was every 1000 generations. The first 10% of sampled trees as burn-in sample and the remaining trees were used for a majority-rule consensus tree and estimating posterior probabilities (PP). The MP analysis was performed in PAUP* version 4.0 beta 10 (Swofford, 2003) which involves the setting of heuristic tree searches with 1000 replications of random sequences entries and tree bisection-reconnection (TBR) branch swapping. Branch support was evaluated by bootstrap analysis with 100 0000 replicates. The ML analysis was conducted using RAxML at the CIPRES Science Gateway (Miller et al., 2010). Node support was assessed using 1000 bootstrap replicates.

2.4. Divergence time estimate

The crown age of the section *Sikkimensia* was estimated using a Bayesian approach based on nrITS with an uncorrelated lognormal relaxed molecular clock model (Drummond et al., 2006), as implemented in Beast 1.75 (Drummond and Rambaut, 2007). Sequences of nrITS were downloaded from GeneBank and newly generated in this study, for 173 samples (include 124 species of *Allium*) representing 46 genera of Amaryllidaceae (Table S4). The Beast analysis was run for 1×10^8 generations with sampling every 10,000 generations and used the GTR + I + G substitution model selection by MrModeltest and randomly generated Starting Tree and the Yule tree prior. In view of the lack of the fossils of *Allium* and a few fossils of the Asparagales have been reported from the late Eocene (Couper, 1960; Muller, 1981; Herendeen and Crane, 1995) may be too young to calibrate the crown clade of the order (Wikström et al., 2001; Janssen and Bremer, 2004), calibration points from previous studies be used in this study. Based on Zanne (2014) and Tank (2015), we calibrated the crown age of the MRCA (Most recent common ancestor) of (Xanthorrhoeaceae) and (Asparagaceae + Amaryllidaceae) as 81.4 Ma, and with a normally distributed standard deviation of 0.1. We also set the crown age of Amaryllidaceae at 51.2 Ma with a normally distributed standard deviation of 2.5 and the crown age of Allioideae at 37 Ma with a normally distributed standard deviation of 4.5 based on Chen (2013).

Subsequently, the divergence times within *Sikkimensia* were estimated separately based on nrDNA and cpDNA datasets using the same methods stated above. The HKY + G substitution model was selected for nrDNA dataset and the GTR + I + G model was selected for cpDNA dataset. The crown age of the section *Sikkimensia* was set to 7.64 Ma based on previous analysis, with a normally distributed standard deviation of 2. According to previous phylogenetic analysis (Friesen et al., 2006; Li et al., 2010), *A. rude* and *A. chrysocephalum* were used to root the tree.

In additionally, the substitution rates were also used to estimate divergence time of the section *Sikkimensia*. Considering the constant cpDNA substitution rates for most angiosperm species have been estimated to be in the range $1–3 \times 10^{-9}$ substitutions per site per year (sub/site/yr) (Wolfe et al., 1987). The mean of 1.52×10^{-9} s/s/y of the chloroplast non-coding regions of grass (Yamane et al., 2006) was chosen as the mutation rates. We used the uncorrelated lognormal relaxed clock (ucld) to estimate the divergence time, by setting nucleotide substitution models from MrModelTest 2.2 (Nylander, 2004) plus gamma distribution, the Yule process speciation and the most suitable tree prior for inferring relationships between major lineages. The MarKov chain Monte Carlo (MCMC) algorithm was run for 2×10^7 generations and sampling every 2000 generations, with four incrementally heated chains. The effective sample size analysis was performed in Tracer 1.6 (http://beast.bio.ed.ac.uk/). The mean and 95% highest posterior (HPD) intervals of ages were accessed by Tree Annotator 2.0 and were viewed in FIGTREE 1.4.0 (http://tree.bio.ed.ac.uk/software/figtree/).

2.5. Ancestral area reconstruction

The ancestral area were reconstructed in RASP version 4.0 (http://mnh.scu.edu.cn/soft/blog/RASP/index.html) (Yu et al., 2015) based on Bayesian Binary Method (BBM) in cpDNA and nrDNA dataset, respectively. We selected the F81 + G rate model, under which the rates of local extinction and dispersal can be underlined during the analysis since unequal rate within and among each distribution range. The BBM analyses ran for 2 million generations using 9 hot Markov chains and 1 cold chain with temperature increments of 0.1. Three distributional areas of the section *Sikkimensia* were delimited according to the floral composition and vegetation types across regions (Wu, 1979; Wu and Wu, 1996). a, Sino-Japanese; b, Sino-Himalayan; c, The QTP*ss*. Distribution areas of all populations in this study were defined according to the distribution of the field observed situation.

2.6. Population genetic, phylogeographic analyses and demographical history

To verify the degrees and patterns of diversity in the nrDNA and cpDNA data within the section *Sikkimensia*, haplotype diversity and nucleotide diversity for each population and at the lineage level were calculated by using DNAsp version 5.0 (Librado and Rozas, 2009). We used the PERMUT (Pons and Petit, 1996) to calculate the level of population differentiation at lineage level (*G*st) and estimate of population subdivision for phylogenetically ordered alleles (*N*st). The U-statistics were used to test the phylogeographical structure between *G*st and *N*st at lineage level. To quantify the genetic differentiation partitioned among different lineages, analyses of molecular variance (AMOVA) (Excoffier et al., 1992) were carried out with the software ARLEQUIN version 3.5 (Excoffier and Lischer, 2010). A maximum parsimony median-joining network among the haplotypes within *Sikkimensia* was obtained by using NETWORK version 4.5 (Polzin and Daneshmand, 2003). To detect whether population lineages within the section *Sikkimensia* experience recent population expansion, mismatch distribution analysis (MDA) was performed by using the ARLEQUIN version 3.5 (Excoffier and Lischer, 2010). The smoothness of observed mismatch distribution was calculates by the sum of squared deviations (SSD) between observed and expected mismatch distributions and Harpending's (1994) raggedness index (H_{Rag}). Additionally, Tajima's *D* and Fu's F_s were calculated in ARLEQUIN version 3.5 (Excoffier and Lischer, 2010).

2.7. Climatic data analysis and test for IBD and IBE

To identify climatic factors which were potentially linked to the genetic structure and divergence in three lineages (lineage A, C and D) within the section *Sikkimensia*, we used recent data (1950–2000) for 19 BioClim variables (Hijmans et al., 2005) from the high-resolution climate layer data with a grid size of 30″ based on our sample locality data (Table 1). We extract the climatic variables by R and use calculated the mean values and standard errors with SPSS version 19 for each population and a two-tailed *t*-test on the three lineages within the section *Sikkimensia* separately.

In order to test the correlation between geographic, climatic and genetic distance, three matrices were built to describe differences between populations within the section *Sikkimensia*. (1) we calculated population-level pairwise genetic differences as $F_{ST}/(1 - F_{ST})$ from nrDNA and cpDNA in ARLEQUIN version 3.5 (Excoffier and Lischer, 2010), respectively; (2) geographic distance was based on data from the latitude and longitude of the site of sample collection; (3) climatic differences calculated as the Euclidian distance between the population means for the two climatic variables from the Principal component analysis (PCA) of climatic variables (the estimates of relative contributions of the environmental variables (above 5) to the Maxent model were selected as available environmental variables for building climatic matrice) (to see Table S6). To test separately whether genetic distance was related to geographic distance and climatic distance, Mantel tests (Smouse et al., 1986; Manly, 1997) were conducted in the Ecodist package in R (Goslee and Urban, 2007), with significance determined via permutation tests. Meanwhile, to control for the potentially confounding effect of hierarchical structure on relationships between distance matrices, the partial Mantel tests were performed in R (Goslee and Urban, 2007).

2.8. Species distribution modeling

To estimate the present and past distribution of the all lineages within the section *Sikkimensia*, SDM was carried out by using MAXENT 3.3.3e (Phillips et al., 2006), and such a modeling were separately tested for three different lineages (lineage A, C and D). We used 339 spatially localities which were obtained from herbarium records in online repositories for analyses (see Table S7). Environmental layers of 19 bioclimatic (Hijmans et al., 2005) variables for the Last Glacial Maximum (LGM, around 21 ka ago) and the current time were downloaded from the WorldClim dataset at 2.5 min resolution and employed for the modeling. The bioclimatic climatic variables with significant effects on the three lineages within the section *Sikkimensia* were used to estimate changes in the distribution ranges of plants, respectively (see Table S6). The parameter setting of a Maxent model is according to the Maxent Model version 3.3.3e Tutorial (Young et al., 2011). The accuracy of each model prediction for each lineage was quantified by calculating the area under the 'receiver operating characteristic (ROC) curve' (AUC) (Peterson et al., 2008; Elith and Leathwick, 2009). AUC values above 0.7 are considered to indicate good model performance (Fielding and Bell, 1997). DIVA-GIS version 7.5 (Hijmans et al., 2001) was performed to draw the range of suitable distributions.

3. Results

3.1. cpDNA data analysis

The combined cpDNA (atpI-atpH, petL-psbE, trnC-rpoB, trnV-ndhC, and trnL-trnF) data has a matrix of 3391 characters across 718 individuals which belong to 79 populations. A total of 56 chlorotypes were identified based on 154 nucleotide polymorphisms (Fig. 1, Tables 1 and S8). The phylogenetic tree (Because of the similar topologies of BI, MP and ML trees, we only displayed the BI tree) and haplotype network (Figs. 3a and 4a) both clustered into four major lineages: (A) distributed across the HMR and the QDM corresponding with morphological characteristic of purple-blue flower and filament and stigma outside perianth pale; (B) only distributed in the southeastern margin of the QDM with similar morphological characteristic to lineage A (Fig. S1); (C) distributed in the QDM and adjacent region featuring pink-white flower and filament and stigma outside perianth pale; (D) largely distributed in the HMR featuring purple-blue flower and filament and stigma within perianth pale. The lineage A included two species (*A. cyaneum* and *A. stenodon)*, but *A. stenodon* were deeply nested within *A. cyaneum* (Fig. 3a). The lineage B also contained two species (*A. henryi* and *A. heteronema*). The lineage C comprised *A. plurifoliatum* var. *plurifoliatum* and *A. paepalanthoides*. The lineage D contained four species (*A. sikkimense*, *A. beesianum*, *A. yuanum* and *A. plurifoliatum* var. *zhegushanense)*, the C1 haplotype was shared by *A. sikkimense* and *A. yuanum*, the C3 haplotype was shared by *A. sikkimense* and *A. beesianum* (Figs. 3a and 4a).

The geographical distribution of the cpDNA haplotypes is shown in Fig. 1. Molecular genetic diversity indices H_d and π for each population are summarized in Table S9, with H_d ranging from 0.000 to 0.733 and π ranging from 0.000 to 0.093. At the lineage level, H_T was higher than H_S for each lineage and seen in Table 2. Additionally, N_{ST} was significantly higher than G_{ST} in all lineages (Table 2), indicating the existence of significant phylogeographical structure in the lineage level.

The AMOVA indicated that 80.1% of genetic variation was generated among lineages, 18.61% among populations within lineages and 1.28% within populations (Table 3). The mismatch distribution analysis (MDA) showed that the three lineages (A, C and D) were multimodal or bimodal, implying that recent population expansion for the three lineages were unlikely (Fig. S2). The neutral test results were not significantly, which displayed that there were no demographic expansion in each lineage in the past (Table 4).

3.2. nrDNA data analysis

The length of aligned sequences was 494 bp for ETS, and 634 bp for ITS. Through the combination of the two datasets, 61 nrDNA haplotypes were recovered based on 207 polymorphic sites (Fig. 2, Tables 1 and S10). Only the Bayesian tree was shown because the BI, MP and ML tree have the same topology (Fig. 3b). The network of nrDNA

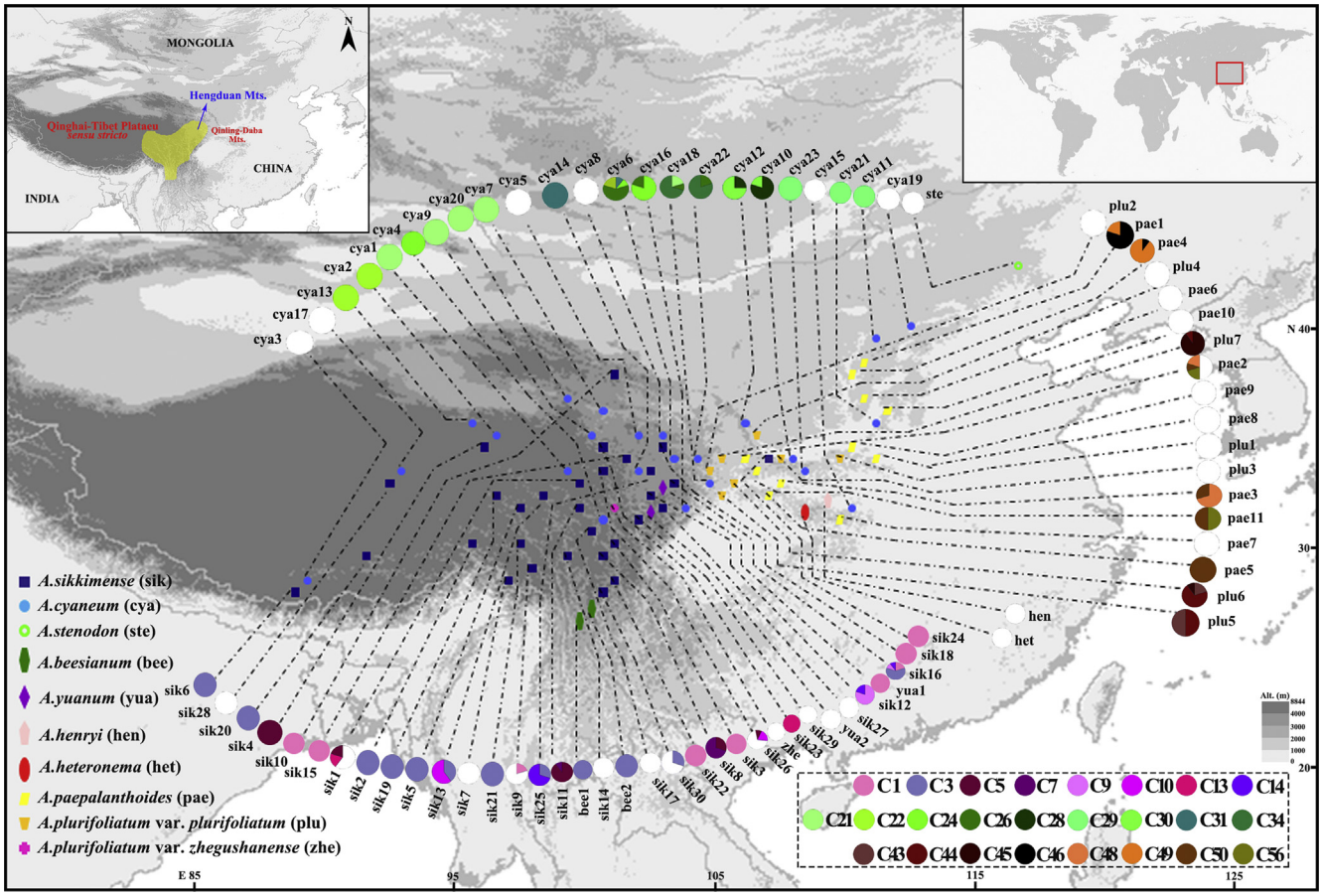

Fig. 1. Map of the sampling locations in Table 1 and the geographic distribution of cpDNA haplotypes detected within the section *Sikkimensia*. All haplotypes that are found in more than one population are color-coded, while private haplotypes are shown in white. Haplotypes colours correspond to those shown in the bottom-right corner.

haplotypes was roughly consistent with the phylogenetic tree and also grouped into four distinct lineages (A, B, C and D) that corresponded to cpDNA data (Figs. 2 and 3b). No nrDNA haplotypes were shared among the ten species but *A. stenodon* was also nested within *A. cyaneum.* Each species formed its own individual branch in nrDNA data.

The geographical distribution from the nrDNA haplotypes is shown in Fig. 2. The H_d ranged from 0.000 to 0.556 and π ranged from 0.000 to 0.763 within total populations (Table S9). Based on nrDNA data, each lineage also displayed the high total genetic diversity and low average within-population genetic diversity (Table 2). Similar to cpDNA, the nrDNA indicated a significant phylogeographical structure at the lineage level.

AMOVA showed that 59.86% of the genetic variation occurred among lineages and that 37.59% of the variation was partitioned among all populations within lineages, and that 2.54% occurred within population (Table 3). The mismatch distribution analysis gave clear multimodal graphs for each lineage (A, C and D), as well as non-significant results of neutrality test, which showed the populations did not undergo expansion in the past (Fig. S2 and Table 4).

3.3. Divergence time estimation and ancestral area reconstruction

Divergence time analyses based on nrITS and three calibration points indicated that the crown group of *Allium* section *Sikkimensia* originated during the late Miocene (approx. 7.64 Ma) (Fig. S3). Subsequently, a normal distribution with a standard deviation of 2 and centered about the median 7.64 Ma was applied to section *Sikkimensia* root node for dating of the nrDNA and cpDNA phylogenies, respectively. The BEAST-derived chronogram of section *Sikkimensia* based on nrDNA dataset recovered the crown age of the section as approx. 7.9 Ma (95% HPD: 5.85–10.3 Ma). The earliest diverging lineage among the four lineages, lineage A, was first separated during the early Pliocene (approx. 5.51 Ma; 95% HPD: 4.0–7.5 Ma). The lineage B was next oldest lineage, dating back to approx 4.58 Ma (95% HPD: 4.0–7.5 Ma) ago. The lineage C and D probably diverged during the middle Pliocene (approx. 3.79 Ma; 95% HPD: 2.64–5.26 Ma) (Fig. S4). Results obtained from the cpDNA dataset BEAST analysis indicated that the crown age of the section *Sikkimensia* was estimated at 9.01 Ma ago (95% HPD: 6.72–11.44 Ma). The first split among the four lineages was around 6.39 Ma (95% HPD 4.56–8.68 Ma). The lineage B was separated around 5.41 Ma (95% HPD: 3.69–7.46 Ma). The divergence time between lineage C and D was around 4.48 Ma (95% HPD: 3.05–6.33 Ma) (Fig. S5). Additionally, molecular dating based on cpDNA substitution rate showed that the crown age of the section *Sikkimensia* was estimated at 5.44 Ma ago (95% HPD: 3.25–8.4 Ma). The first divergence among the four lineages was around 4.42 Ma (95% HPD 2.71–6.4 Ma). The lineage B was separated around 3.64 Ma (95% HPD: 2.26–5.35 Ma). The split between lineage C and D was around 2.85 Ma (95% HPD: 1.78–4.24 Ma). In view of the result of the crown age of the section *Sikkimensia* based on nrDNA dataset was closed to the time that estimated by nrITS dataset (7.9 Ma versus 7.64 Ma) (Figs. S3 and S4), we selected the results of molecular dating based on nrDNA dataset to explain the biogeographic history of *Allium* section *Sikkimensia* (Figs. 5 and S6).

The results of ancestral area reconstruction based on cpDNA dataset indicated that the initial differentiation center of the section *Sikkimensia* was most likely distributed in the HMR (node I). A part of ancestral population colonized to the east from the ancestral area, and diversified

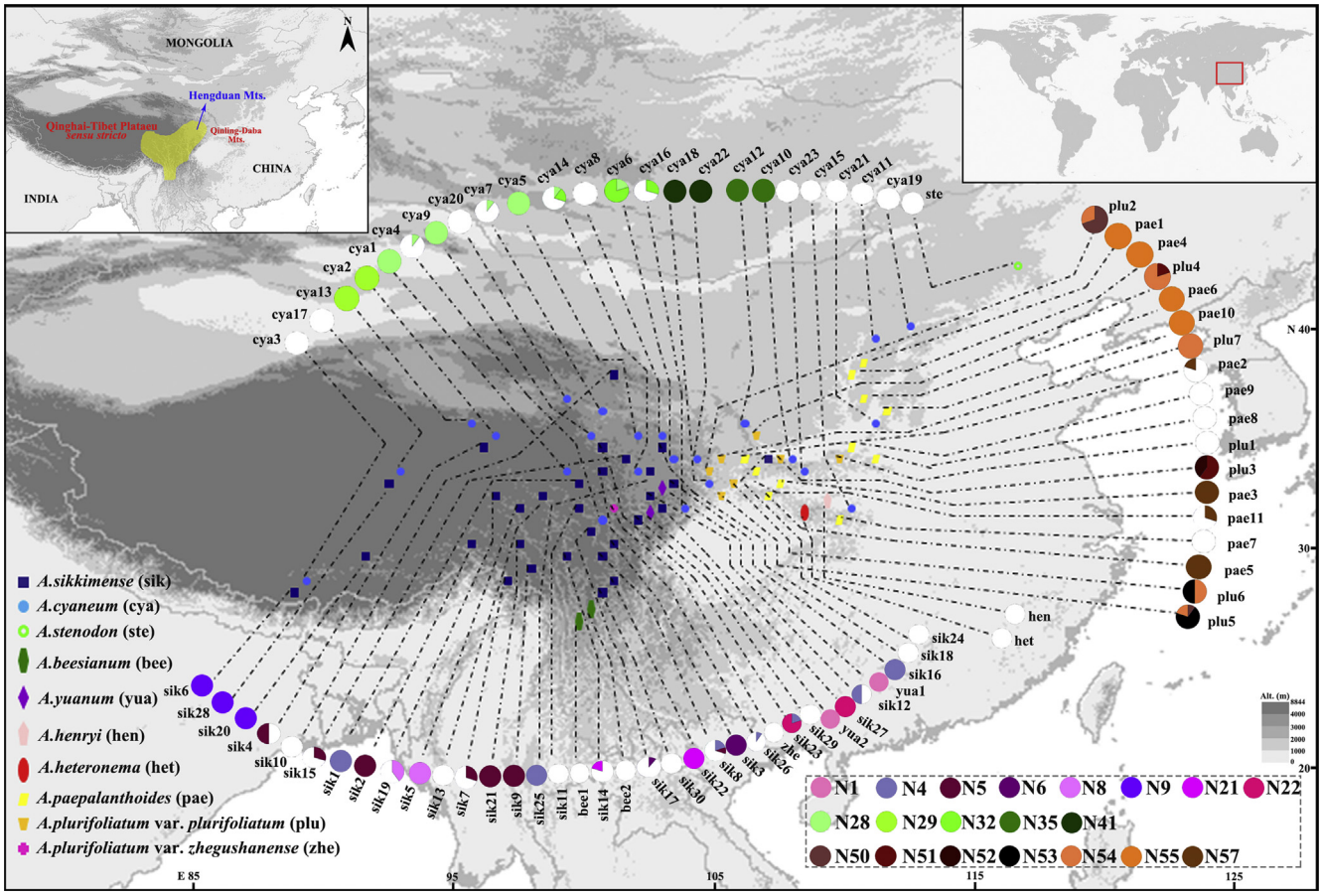

Fig. 2. Map of the sampling locations in Table 1 and the geographic distribution of nrDNA haplotypes detected within the section *Sikkimensia*. All haplotypes that are found in more than one population are color-coded, while private haplotypes are shown in white. Haplotypes colours correspond to those shown in the bottom-right corner.

in QDM and adjacent region during the late Miocene to early Pliocene (Fig. 5a). The BBM analyses identified a dispersal event from the HMR to the QDM during the late Miocene (node I), suggesting colonization from the cold highlands to the warm lowlands. Meanwhile, two main dispersal events from the QDM to the HMR (node IV and node VII) during the middle Pliocene were identified by BBM analysis, reflecting colonization from the warm lowlands to cold highlands. BBM analysis based on the topology of the nrDNA chronogram resulted in similar reconstructions to cpDNA results (Fig. S6).

3.4. Climatic data and the results of correlation test

Out of the 19 climatic variables, all but five (bio7: temperature annual range, bio9: mean temperature of driest quarter, bio13: precipitation of wettest month, bio16: precipitation of wettest quarter, bio18: precipitation of warmest quarter), showed significant differences in mean values between population of the lineage C and D (Table 5). Compared with lineage C and D separately, the lineage A exhibited significant differences in the 9 temperature variables, but only bio15 (precipitation seasonality) as a precipitation variable showed significant differences between lineage A and C.

The results of Simple Mantel test revealed significant correlations ($P \leq 0.001$) between the genetic (from cpDNA and nrDNA data, respectively) and geographic matrices ($r = 0.383$, $P = 0.001$; $r = 0.344$, $P = 0.001$), but no significant correlations between genetic and climatic matrices ($r = 0.279$, $P = 0.004$; $r = 0.23$, $P = 0.018$) in lineage A (Figs. S7 and S8). The partial Mantel test also displayed that Pairwise genetic and geographic distance matrices were strongly correlated when controlling for climatic effects in lineage A ($r = 0.302$, $P = 0.001$; $r = 0.319$, $P = 0.001$). However, a no significant correlation was observed between genetic distance and climatic distance, after controlling for geographic structure (Table 6). These results indicated that genetic differentiation in lineage A may be influenced by geographic distance rather than climatic factor. Moreover, there were non-significant correlations between the genetic and geographic matrices, genetic and climatic matrices in lineage C (Fig. S7 and S8). Meanwhile, in lineage D, the results of the Simple and partial Mantel test based on two type genetic matrices separately is similar to lineage C. In addition, we detected significant correlation between genetic and geographical matrices ($r = 0.262$, $P = 0.001$; $r = 0.278$, $P = 0.001$), and between genetic and climatic matrices ($r = 0.279$, $P = 0.001$; $r = 0.251$, $P = 0.001$) based on the combined data from two lineages (C and D), even when controlling for climatic and geographical effect separately (see Table 6). This result indicates that IBD and IBE both influenced the genetic structure of the lineage C + D.

3.5. Species distribution modeling

We modeled the distribution of four groups (all four lineages, lineage A, C and D) under two climate scenarios (the current and the LGM). All models had high predictive power (AUC > 0.95), indicating the relationship was not random. Present distribution predictions were universally nice representations of the actual distributions of the four groups (Fig. 6). For the all four lineages within the section *Sikkimensia*, the HMR part of its potential species range was intense contracted, however, there was an obvious expansion in the QDM region in the LGM. During the LGM, lineage A showed contraction of distribution range in the HMR and expansion in the QDM. The lineage C displayed

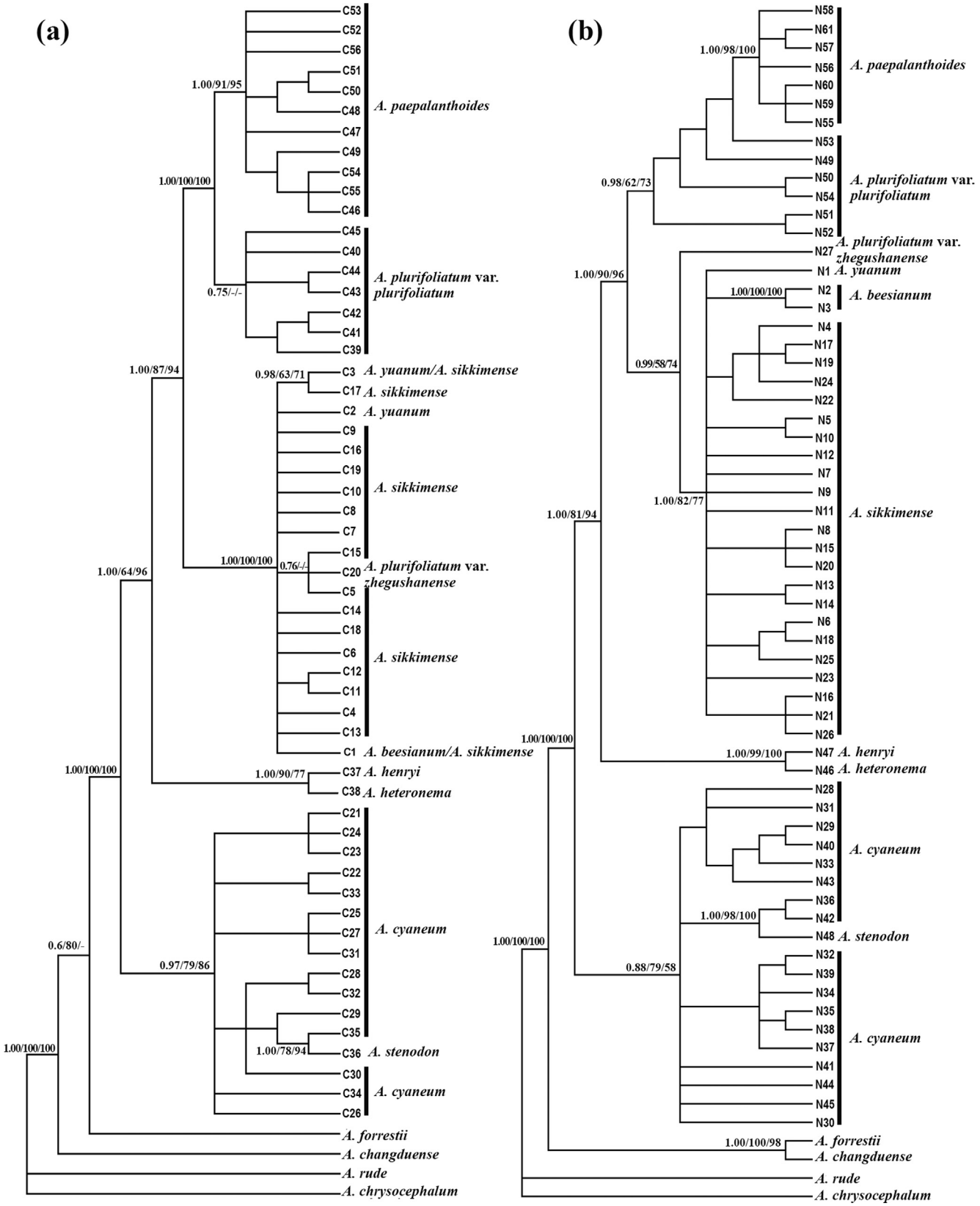

Fig. 3. Phylogenetic relationship of the studies taxa within the section *Sikkimensia* recovered from the chlorotypes (a) and ribotypes (b). The Bayesian inference (BI) trees were only shown for the similar topologies with maximum parsimony (MP) and maximum likelihood (ML) tree. Posterior probabilities (> 50%) and bootstrap support values (> 50%) from BI/MP/ML analyses above branches. Short line denotes the values below 50%.

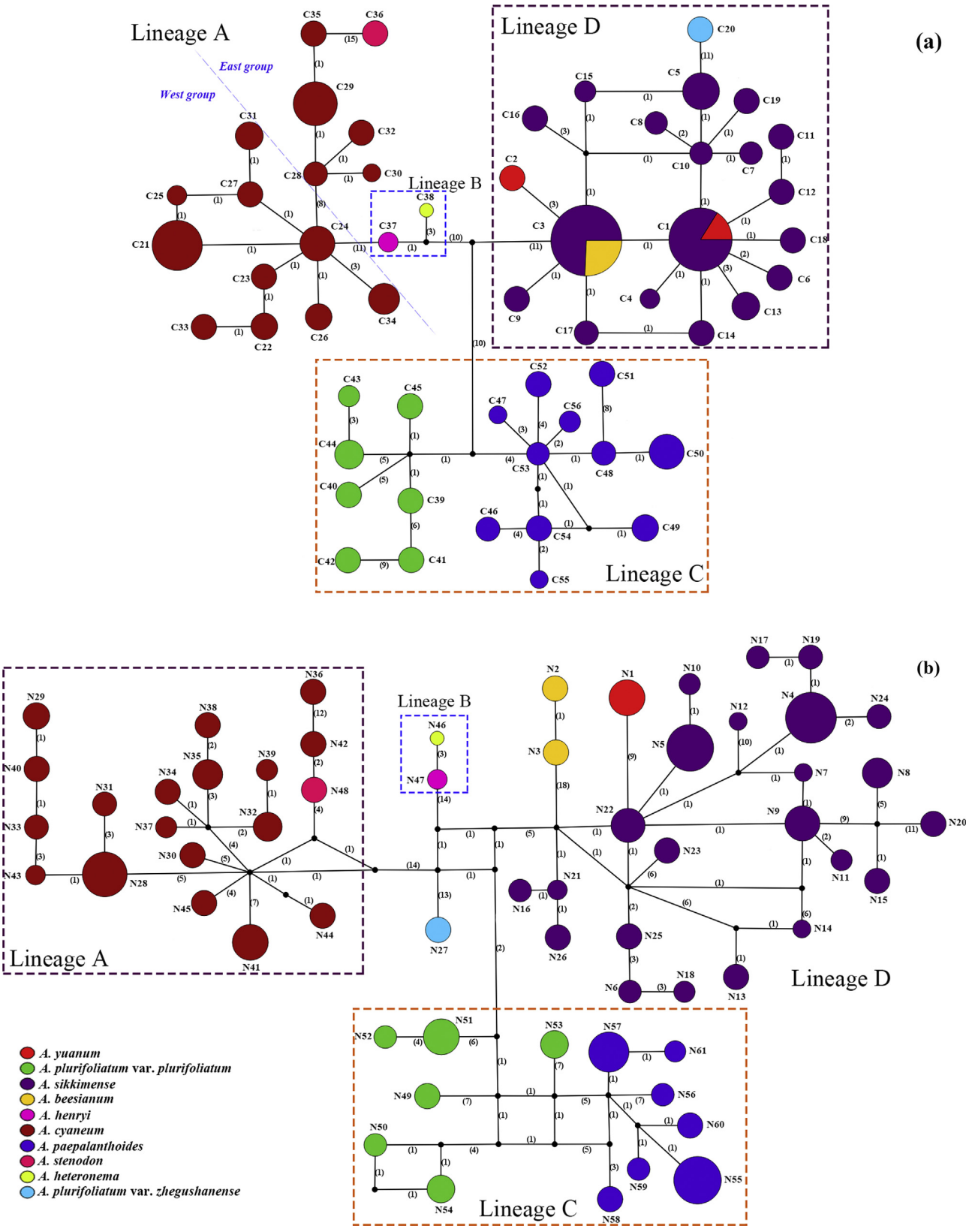

Fig. 4. MP median-joining network based on (a) 56 cpDNA haplotypes and (b) 61 nrDNA haplotypes within the section *Sikkimensia*. Each color represents the studies taxa. The size of circles in the network corresponds to the frequency of each haplotype. Numbers in the brackets on branches indicate the number of mutations between haplotypes. Small solid black circles denoted hypothetic unsampled or extinct ancestral haplotypes.

Table 2
Genetic diversity and genetic differentiation of 79 populations within *Allium* section *Sikkimensia* at lineage level.

Lineages	H_S	H_T	G_{ST}	N_{ST}
cpDNA				
Lineage A	0.118 (0.0441)	0.965 (0.0155)	0.877 (0.0454)	0.942 (0.023)
Lineage B	/	/	/	/
Lineage C	0.199 (0.0608)	0.985 (0.0061)	0.798 (0.0629)	0.918 (0.0291)
Lineage D	0.119 (0.0365)	0.913 (0.029)	0.87 (0.0387)	0.924 (0.0317)
Total	0.132 (0.025)	0.974 (0.0083)	0.864 (0.0255)	0.984 (0.0035)
nrDNA				
Lineage A	0.075 (0.0331)	0.968 (0.0156)	0.922 (0.0341)	0.965 (0.02)
Lineage B	/	/	/	/
Lineage C	0.18 (0.056)	0.933 (0.0318)	0.807 (0.058)	0.888 (0.0451)
Lineage D	0.117 (0.0333)	0.973 (0.011)	0.879 (0.0342)	0.927 (0.0291)
Total	0.115 (0.022)	0.988 (0.003)	0.884 (0.0222)	0.968 (0.0087)

Average gene diversity within populations (H_S), total gene diversity (H_T), interpopulation differentiation (G_{ST}), and number of substitution typed (N_{ST}).

an extensive expansion in the QDM and adjacent region during the LGM. The palaeoclimate data modeling for lineage D showed an extensive constriction in the HMR, but a slight expansion in the western margin of the QDM.

4. Discussion

4.1. Relationships among species

With extensive and accurate sampling strategy, our phylogenetic analysis support the earlier finding that the section *Sikkimensia* is monophyletic clade and comprises two major groups (Li et al., 2010). One group contained two species (*A. forrestii* and *A. changduenes*), while another group included the remaining ten species. In this paper, discussion was focused on the latter group. The phylogenetic tree based on the robitype displayed a clear resolution for this group that each species formed a clade, but *A. stenodon* nested in the clade of *A. cyaneum* (as well as in the chlorotype tree) (Fig. 3a and b). Based on the contrast of the original description in detail and the extensive observations in the wild, we find that the two taxa possess similar habitat and morphological traits (Fig. S1 and Table S2). In addition, the key trait for distinguishing the two taxa is that the inner filaments broadened at base and with 1 long tooth on each side for *A. stenodon*, while *A. cyaneum* showed the similar trait that the inner ones broadened at base and base sometimes 1-toothed on each side. Besides, *A. cyaneum* occurs in the wider altitude range (1992–4370 m) than *A. stenodon* (about 2000 m). Moreover, the geographical distribution region of *A. stenodon* is close to the northeastern populations (cya11 and cya19) of the total geographical range of *A. cyaneum* (Figs. 1 and 2). Thus, combining the molecular phylogentic analysis, *A. stenodon* seems to be an ecotype of *A. cyaneum*.

However, a little phylogenetic incongruence was detected between the nrDNA and cpDNA data sets. In the chlorotype tree, *A. beesianum, A. yuanum*, *A. plurifoliatum* var. *zhegushanense* and *A. sikkimense* shared a common branch, and *A. yuanum* and *A. beesianum* separately shared chlorotype with *A. sikkimense* (C3 and C1) (Figs. 3a and 4a). In general, incongruence between the different typical gene trees may have resulted from incomplete lineage sorting (ILS) and hybridization/introgression (Degnan and Rosenberg, 2009; Shahzad et al., 2017). ILS, which is one scenario of the persistence of ancestral polymorphisms through speciation events, may have led to the sharing of genotypes among species (Avise, 2000; McGuire et al., 2007). The coalescence of organelle DNA is four times faster in lineage sorting than nuclear genes (Moore, 1995), and it is unlikely that the lineage sorting for nuclear gene had been completed if the lineage sorting for chloroplast gene is not yet complete. In consideration of the nrDNA tree is fit well in morphology and thus seemed finished lineage sorting, we think ILS is likely insufficient to explain the gene-tree incongruence. Parapatric/sympatric geographic distribution may create the chances for hybridization and introgression among species (Anderson, 1949; Rautenberg et al., 2010; Du et al., 2011). The chlorotypes C1 and C3 were separately found in the parapatric populations of *A. yuanum*, *A. beesianum* and *A. sikkimense* (Fig. 1). Meanwhile, our field observation

Table 3
Analysis of molecular variance (AMOVA) based on the cpDNA and nrDNA data.

	Source of variation	*d.f.*	*SS*	*VC*	*PV* (%)	Fixation indices
cpDNA						
All lineages	Among lineages	3	5981.314	12.603	80.1	FSC: 0.935**
	Among populations within lineages	75	2019.401	2.928	18.61	FST: 0.987**
	Within population	639	128.75	0.201	1.28	FCT: 0.801**
Lineage A	Among populations	23	592.141	2.977	94.23	FST: 0.942**
	Within population	193	33.55	0.182	5.77	
Lineage B	Among populations	/	/	/	/	
	Within population	/	/	/	/	
Lineage C	Among populations	17	833.463	5.057	91.56	FST: 0.915**
	Within population	155	72.3	0.466	8.44	
Lineage D	Among populations	34	524.124	1.677	91.97	FST: 0.919**
	Within population	284	41.6	0.146	8.03	
All samples	Among populations	78	8000.715	11.269	98.24	FST: 0.982**
	Within population	639	128.75	0.201	1.76	
nrDNA						
All lineages	Among lineages	3	4225.703	8.753	59.86	FSC: 0.936**
	Among populations within lineages	75	3789.87	5.497	37.59	FST: 0.974**
	Within population	639	237.5	0.371	2.54	FCT: 0.598**
Lineage A	Among populations	23	1174.278	5.916	96.16	FST: 0.961**
	Within population	193	43.5	0.236	3.84	
Lineage B	Among populations	/	/	/	/	
	Within population	/	/	/	/	
Lineage C	Among populations	17	857.801	5.184	88.49	FST: 0.884**
	Within population	155	104.5	0.674	11.51	
Lineage D	Among populations	34	1687.961	5.412	93.52	FST: 0.935**
	Within population	284	106.5	0.375	6.48	
All samples	Among populations	78	8015.574	11.272	96.81	FST: 0.968**
	Within population	639	237.5	0.371	3.19	

F_{CT} = differentiation among groups; F_{ST} = differentiation among populations; F_{SC} = differentiation among populations within groups. ** $P < 0.001$.

Table 4
Results of the mismatch distribution analysis and neutrality tests for the main lineages and all lineages within *Allium* section *sikkimensia* recognized by phylogenetic inferences.

	Tajima's *D*(*p*)	Fu's F_S(*p*)	*Tau*	Expansion time (t,Ka)	MDA	SSD(*p*)	*H*rag(*p*)
cpDNA							
Lineage A	–0.01091 (0.88174)	0.44400 (N.A.)	0.66406 (± 1.40748)	NC	Bimodal	0.04883 (0.03565)	0.13273 (0.12522)
Lineage B	/	/	/	/	/	/	/
Lineage C	0.07244 (0.80122)	1.36920 (N.A.)	1.40061 (± 2.00602)	NC	Multimodal	0.07982 (0.02883)	0.25841 (0.19167)
Lineage D	0.11299 (0.92197)	0.3417 (N.A.)	0.71802 (± 1.39477)	NC	Bimodal	0.02875 (0.05826)	0.12566 (0.09471)
All	0.06247 (0.89044)	0.48983 (N.A.)	1.21049 (± 4.59933)	NC	Multimodal	0.03591 (0.06342)	0.14204 (0.12595)
nrDNA							
Lineage A	−0.16116 (0.85048)	0.63164 (N.A.)	0.42154 (± 1.00858)	NC	Multimodal	0.02998 (0.01348)	0.12240 (0.13609)
Lineage B	/	/	/	/	/	/	/
Lineage C	0.42555 (0.93028)	1.77649 (N.A.)	0.81510 (± 1.51179)	NC	Multimodal	0.10827 (0.031)	0.25325 (0.18544)
Lineage D	0.09827 (0.88563)	0.98235 (N.A.)	0.44135 (± 1.04536)	NC	Multimodal	0.07376 (0.02363)	0.18682 (0.18746)
All	0.08976 (0.88994)	0.96486 (N.A.)	0.61056 (± 1.58984)	NC	Multimodal	0.06111 (0.02557)	0.16788 (0.15987)

Sum of squared deviation under expansion model (SSD), Harpending's raggedness index (*H*rag). Not calculate (NC).

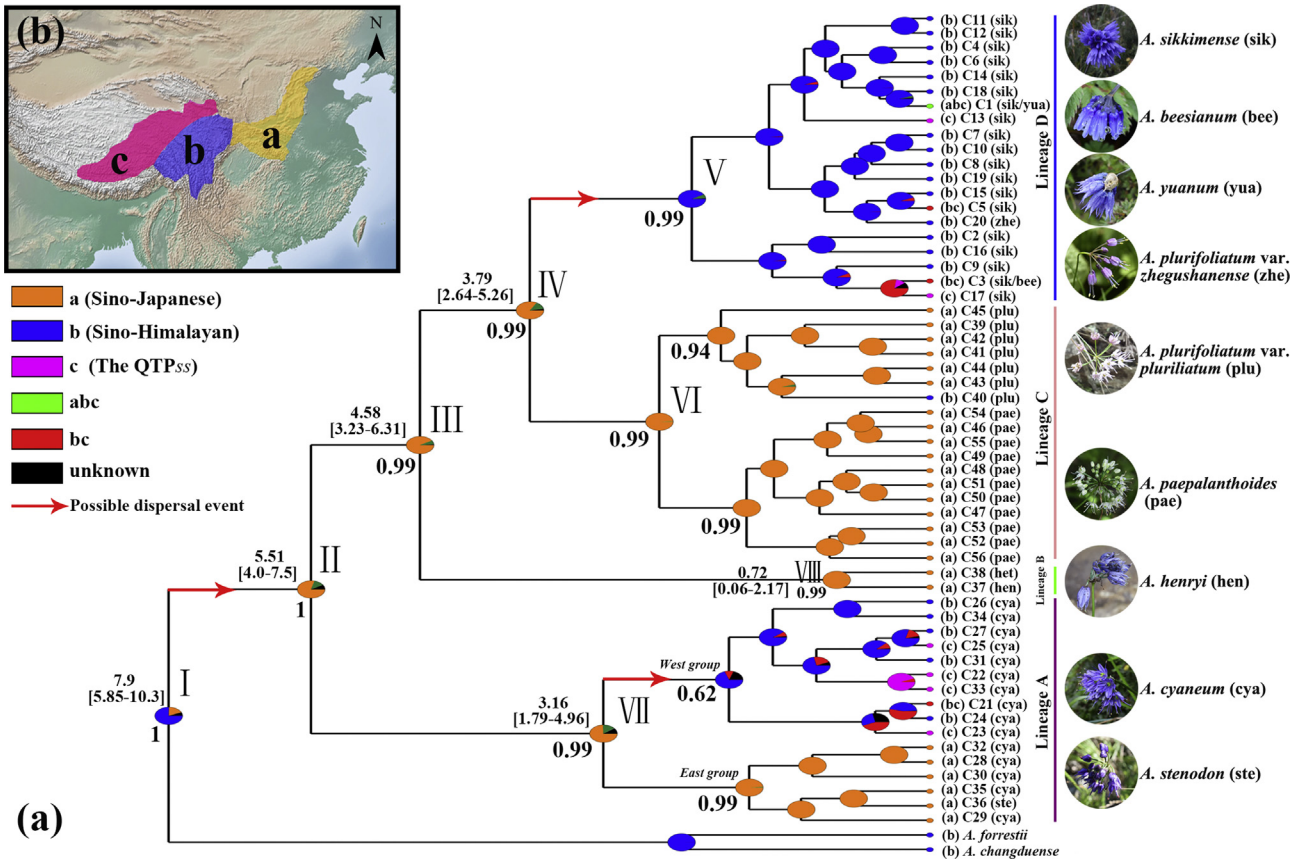

Fig.5. Ancestral area reconstructions based on the cpDNA phylogeny within the section *Sikkimensia*. (a) Pie charts show proportions of the ancestral ranges. The divergence time (in Ma) of the main nodes based on nrDNA dataset. Numbers in the brackets show the 95% HPD of divergence time (in Ma) of the main nodes. Numbers below branches in the Bayesian tree are posterior probability values. Photographs to the right show the flower of each study taxa (except for *A. heteronema*). (b) The insert map shows three floristic divisions (a–c) in China according to Wu and Wu (1996).

showed that the three species have overlapping flowering times and similar morphological trait of flower (purple-blue flower color and filament and stigma within perianth pale), which might have accelerated genetic introgression among these species. The occurrence of hybridization among species distributed in same region and subsequent backcrosses with one of the parental species could result in shared chlorotype (Raamsdonk et al., 1997; Li et al., 2013; Wang Z et al., 2014; Li et al., 2016). Hence, as there was no much taxonomic confusion in nrDNA, we suggest that the result of chloroplast capture from the maternal species at population level may be the main reason for the gene-tree discordance in this study.

In addition, the phylogenetic position of *A. plurifoliatum* var. *zhegushanense* is very interesting. It showed close relationship to *A. sikkimense*, but similar to *A. plurifoliatum* var. *plurifoliatum* in morphology. In field survey, in spite of the fact that *A. plurifoliatum* var. *zhegushanense* is distributed in higher average altitude (3350 m) than *A. plurifoliatum* var. *plurifoliatum* (2140 m), the two species both inhabit shady and moist slope in forest margins (Table S2). So, this case may be ascribed to phenotypic convergence under similar selection strategy in the similar habitat (Yuan et al., 2008).

Table 5
Mean, standard errors (SE) and results of *t*-test on 19 BioClim variables for 79 populations for the main lineages within the section *Sikkimensia*.

Lineage		Average Altitude (m)	Bio1 (°F)	Bio2 (°F)	Bio3 (°F)	Bio4 (SD*100)	Bio5 (°F)	Bio6 (°F)	Bio7 (°F)	Bio8 (°F)	Bio9 (°F)	Bio10 (°F)	Bio11 (°F)	Bio12 (mm)	Bio13 (mm)	Bio14 (mm)	Bio15 (CV)	Bio16 (mm)	Bio17 (mm)	Bio18 (mm)	Bio19 (mm)
All populations (two-tailed *t*-test)																					
A	Mean	3015	37	131	36	7850	199	−160	359	129	−68	132	−70	634	128	5	88	345	18	336	18
	SE	750	5	29	7	1398	20	30	44	20	19	20	18	243	38	5	14	99	17	90	17
C	Mean	1816	64	98	29	8010	221	−109	330	154	−44	164	−44	805	152	8	76	412	29	382	29
	SE	342	5	23	5	1189	19	24	40	13	16	17	16	204	27	5	9	76	15	67	15
	P	< 0.001	< 0.001	< 0.01	< 0.01	ns	< 0.001	< 0.001	ns	< 0.001	< 0.001	< 0.001	< 0.001	ns	ns	ns	< 0.05	ns	ns	ns	ns
C	Mean	1816	64	98	29	8010	221	−109	330	154	−44	164	−44	805	152	8	76	412	29	382	29
	SE	342	5	23	5	1189	19	24	40	13	16	17	16	204	27	5	9	76	15	67	15
D	Mean	3815	32	139	42	6380	173	−151	324	108	−51	109	−55	676	141	3	91	385	15	383	15
	SE	435	3	18	4	894	20	23	41	10	14	11	13	186	41	2	10	106	7	106	7
	P	< 0.001	< 0.001	< 0.001	< 0.001	< 0.001	< 0.001	< 0.001	ns	< 0.001	ns	< 0.001	< 0.05	< 0.05	ns	< 0.001	< 0.001	ns	< 0.001	ns	< 0.001
A	Mean	3015	37	131	36	7850	199	−160	359	129	−68	132	−70	634	128	5	88	345	18	336	18
	SE	750	5	29	7	1398	20	30	44	20	19	20	18	243	38	5	14	99	17	90	17
D	Mean	3815	32	139	42	6380	173	−151	324	108	−51	109	−55	676	141	3	91	385	15	383	15
	SE	435	3	18	4	894	20	23	41	10	14	11	13	186	41	2	10	106	7	106	7
	P	< 0.001	< 0.001	ns	< 0.001	< 0.001	< 0.001	ns	< 0.05	< 0.001	< 0.05	< 0.001	< 0.01	ns	ns	ns	ns	ns	ns	ns	ns

Not significant (ns.)

4.2. Geological and ecological factor promote the differentiation within *Sikkimensia*

The impact of orogeny and climate development during recent geological history (i.e. tens of millions of years) on species diversification have been a central topic of debate for years, especially the QTP*sl* uplift event likely has acted a crucial role in the evolutionary history of organisms (Favre et al., 2015). In present study, the strong population genetic structure was identified within the section *Sikkimensia*, for both cpDNA and nrDNA data revealed four distinct lineages (A, B, C and D) that correspond to three various distribution ranges (lineage A: across the HMR and the QDM; lineage B and C: the QDM and adjacent region; lineage D: the HMR) (Fig. 4 and Table 2). Meanwhile, taking together our molecular dating and the ancestral area reconstructions, the results indicated that the initial split of section *Sikkimensia* spanning over the HMR at approximately 7.9 Ma (95% HPD, 5.9–10.3 Ma) (Fig. 5a). During this time, the rapid QTP*sl* uprising was in progress, particularly at eastern fringe, involving several mountain ranges and include the HMR biodiversity hotspot (Harrison et al., 1992; Mulch and Chamberlain, 2006; Royden et al., 2008). Furthermore, the QTP*sl* uplift during the late Miocene might have triggered onset of the Indian and east Asian monsoonal system, and had caused large scale environmental changes in the QTP*sl* and surrounding area (An et al., 2001). The BBM analyses indicated a high probability of the HMR as the ancestral area for the common ancestor of the four lineages (node II). Consequently, a dispersal event at node I strongly suggested that the dispersal from the HMR to the QDM and adjacent region for the common ancestor of the four lineages may have been driven by climate changes following the uplifts of the QTP*sl*. Moreover, this uplift event altered the climate from warm to cold in the HMR, which played as a barrier to distribution and resulted in lineage divergence and speciation in the HMR characterized cold and its eastern adjacent area (QDM) characterized warm. Thus, it may imply that the initial split of section *Sikkimensia*, involving 'cold-warm colonization', was a respond to the QTP*sl* uplift.

We dated the crown node of the lineage C and D (mean 3.79 Ma, 95% HPD: 2.64–5.26 Ma), to the Middle-Late Pliocene (Fig. 5a). This time range would be close to a putative abrupt intensifying of the Asian monsoon regimes around 2.6–3.6 Ma (An et al., 2006; Zhang et al., 2012) which is strongly linked with the intense uplift of the HMR around 3–4 Ma (Chen, 1992, 1996; Shi et al., 1998; Sun et al., 2011; Favre et al., 2015). Moreover, the results of ancestral area reconstruction indicated that possibility of the QDM and adjacent region being the ancestral area for the common ancestor of the lineage C and D is quite high (Fig. 5a). Therefore, the dispersal event at node IV (Fig. 5a) strongly suggested that this split could have occurred during the colonization of the newly available climate and terrain by the species. Additionally, the ancestral chlorotype (C3) of lineage D had a wide distribution range (Figs. 1 and 4a), in conjunction with the C3 detected in Jiuzhaigou which was located in the eastern fringe of the HMR (Fig. 1), suggested that its current distribution range could have been colonized by a single ancient haplotype from the QDM and adjacent region to the HMR. It is true that sik24 was collected in the QDM and adjacent region which was out of the main distribution area of lineage D, but it is probably due to rare seed dispersal events from the HMR to the QDM region. Indeed, our climatic variables analysis between lineage C and D showed that the population of lineage D occurred in the colder and drier climate (Table 5). Furthermore, the results of Mantel test and Partial Mantel test in genetic and climatic distance supported that climatic differences may have played an important role in driving the genetic differentiation for lineage C and D (Table 6 and Fig. S8). Hence, these results indicated that the lineage D may be stem from a dispersal event from warm to cold region following the HMR uplift. In other words, the monsoons (such as Pacific Ocean and Indian monsoons) were blocked by the HMR uplift, henceforth the climate for the HMR being characterized as colder than ever (Kou et al., 2006; Yao et al., 2012; Liu et al., 2013). Thus the 'warm-cold colonization' of the

Table 6
Correlations between genetic $\{F_{ST}/(1 - F_{ST})\}$, cliamatic (from principal component analysis), and Geographic (km) differences among main lineages within the section *Sikkimensia* tested with simple and partial Mantel tests.

	Lineage A		Lineage C		Lineage D		Lineage C + D	
cpDNA								
Simple Mantel test	*r*	*P*-value	*r*	*P*-value	*r*	*P*-value	*r*	*P*-value
Genetic, Geographic	0.383	0.001	−0.101	0.224	0.233	0.004	0.262	0.001
Genetic, Climate	0.279	0.004	−0.011	0.503	0.248	0.004	0.279	0.001
Partial Mantel test								
Genetic, Geographic|Climate	0.302	0.001	−0.096	0.225	0.107	0.051	0.197	0.001
Genetic, Climate|Geographic	0.084	0.177	0.141	0.157	0.16	0.012	0.174	0.001
nrDNA								
Simple Mantel test	*r*	*P*-value	*r*	*P*-value	*r*	*P*-value	*r*	*P*-value
Genetic, Geographic	0.344	0.001	0.031	0.443	0.197	0.024	0.278	0.001
Genetic, Climate	0.230	0.018	0.081	0.325	0.141	0.093	0.251	0.001
Partial Mantel test								
Genetic, Geographic|Climate	0.319	0.001	−0.011	0.474	0.175	0.002	0.249	0.001
Genetic, Climate|Geographic	0.099	0.136	0.129	0.161	0.049	0.239	0.099	0.034

lineage D showed that a respond from the alpine herbal species to the novel habitats and climate regimes following the abrupt HMR uprising.

Based on the cpDNA phylogeny, we estimated the divergence time between two groups (west group versus east group) within the lineage A to have occurred around 3.16 Ma (95% HPD: 1.79–4.96 Ma) (Fig. 5a). The coincidence between this divergence time and the period of intense uplift of the HMR (Sun et al., 2011; Favre et al., 2015), together with the absence of the long-distance dispersal ability in *Allium* (Friesen et al., 2000), suggested that the increasing altitude difference between the HMR and the QDM may limit seed exchange between populations in lineage A. However, we have not detected the similar west-east genetic structure within lineage A based on the nrDNA phylogeny (Fig. S6). Furthermore, in contrast to the fact that the lineage C and D restricted to either area of the HMR and the QDM respectively displayed distinct morphological characteristics, the lineage A showed stable morphological traits through the two areas (Figs. 2 and S1). Because of the high diversity of nrDNA haplotypes, we dismissed the influence from the homogenization of nrDNA (Álvarez and Wendel, 2003). In view of the plant of the lineage A are distributed in grass of high-altitude area (above 1992 m), the open and windy environment is conducive to the spread of pollen, which will enhance gene flow between the HMR and the QDM. Thus, the pollen flow may play an important role to obscure the population genetic structure in nrDNA (Du et al., 2017). Moreover, the fact that a no significant correlation was observed between genetic and climatic distance in lineage A, in conjunction with significant correlations between the genetic and geographic distance, suggested that genetic structure in lineage A may be influenced by geographic factor rather than climatic factor (Table 6). Therefore, such a scenario from the lineage A indicated a respond from the alpine herbal species to altitude difference between the HMR and the QDM following the extensive uplift of the Hengduan Mountains during the late Pliocene.

4.3. Population and range dynamics within Sikkimensia

Climate oscillations during Pleistocene had a prominent effect on species distribution ranges, causing migration and/or extinction of populations (Comes and Kadereit, 1998; Taberlet et al., 1998; Hewitt, 2004). It is widely acknowledged that plant groups have shifted latitude or altitude range in response to the quaternary climate changes (Davis and Shaw, 2001). Our Maxent modeling results for section *Sikkimensia* showed a larger distribution range of this section at the QDM compared to the HMR during the LGM (Fig. 6). This result can be explained partly by the difference of topoclimatic characteristics between the QDM and the HMR. Because the HMR prevents the westward flow of the Pacific Ocean monsoons, the QDM is characterized by a warmer and wetter climate than the HMR, which would provide a more stable environment for plant populations, even during glaciations. In addition, the QDM region shows a relatively simple terrain compared to the HMR (Li and Fang, 1999; Wu et al., 2001). Thus, section *Sikkimensia* populations could have migrated downward and peripherad to track their optimal ecological conditions during the glacial period. By contrast, the HMR featuring highly rugged mountain ranges and deep gorges, could possibly provide multiple refuge for section *Sikkimensia* populations during the quaternary climatic oscillations.

For lineage A, the results from the past (LGM) and present distribution modeling, indicated that the broad-scale distributions (across the HMR and the QDM) of alpine herbal species was lopsided (Fig. 6). In contrast with the obvious range contraction in the HMR, a remarkable range expansion was detected in the QDM region during the LGM. Our mismatch distribution analysis exhibited a ragged bimodal/multimodal distribution in cpDNA and nrDNA data set, in conjunction with the non star-like haplotype structure in the network, which suggested that lineage A had not experienced recent demographic expansion events. These results also indicated that the response of the plant spanning over the HMR and the QDM to the quaternary climate changes was more complicated than previously thought. Additionally, a high level of genetic diversity (Fig. 1 and Table 1) had been detected in Jiuzhaigou (population cya6) and Tanchang (population cya18), which suggested that the eastern fringe of the HMR might be regarded as a glacial refuge for the population of lineage A in the HMR. This area had been regarded as important glacial refuge for the QTP*sl* endemics (Chen et al., 2008; Shahzad et al., 2017). By contrast, range expansion that detected in the QDM may be caused by the fact that the QDM region possesses a lower average altitude than the HMR (Fig. 1). Mountain areas at low altitudes can provide relatively stable environmental conditions to promote expansion/local persistence of species in the Quaternary ice period (Cun and Wang, 2010; Qu et al., 2014).

The lineage C showed a strong range expansion in the past (LGM) distribution modeling (Fig. 6). In general, the cold-tolerant species in high altitude area could undergo range expansion in the LGM (Liu et al., 2013; Shahzad et al., 2017). Interestingly, compared to the lineage A and D distributed in alpine meadow, lineage C is inhabited under the forest which had lower altitude distribution (average altitude: 1816 m) and prefer warm and humid environment (Table 5). This relatively unusual scenario can be explained partly by the low altitude areas of the QDM (as the main distribution area for lineage C) may have provided relative stable environmental conditions during the last glacial period. Previous studies have shown that the QDM and adjacent region had acted as an important refuge for temperate forests species in during these glacial periods (Qian and Ricklefs, 2000; Tian et al., 2009; Bai et al., 2010), which proved that the QDM had relative stable environment during the LGM. Furthermore, the high level of genetic diversity

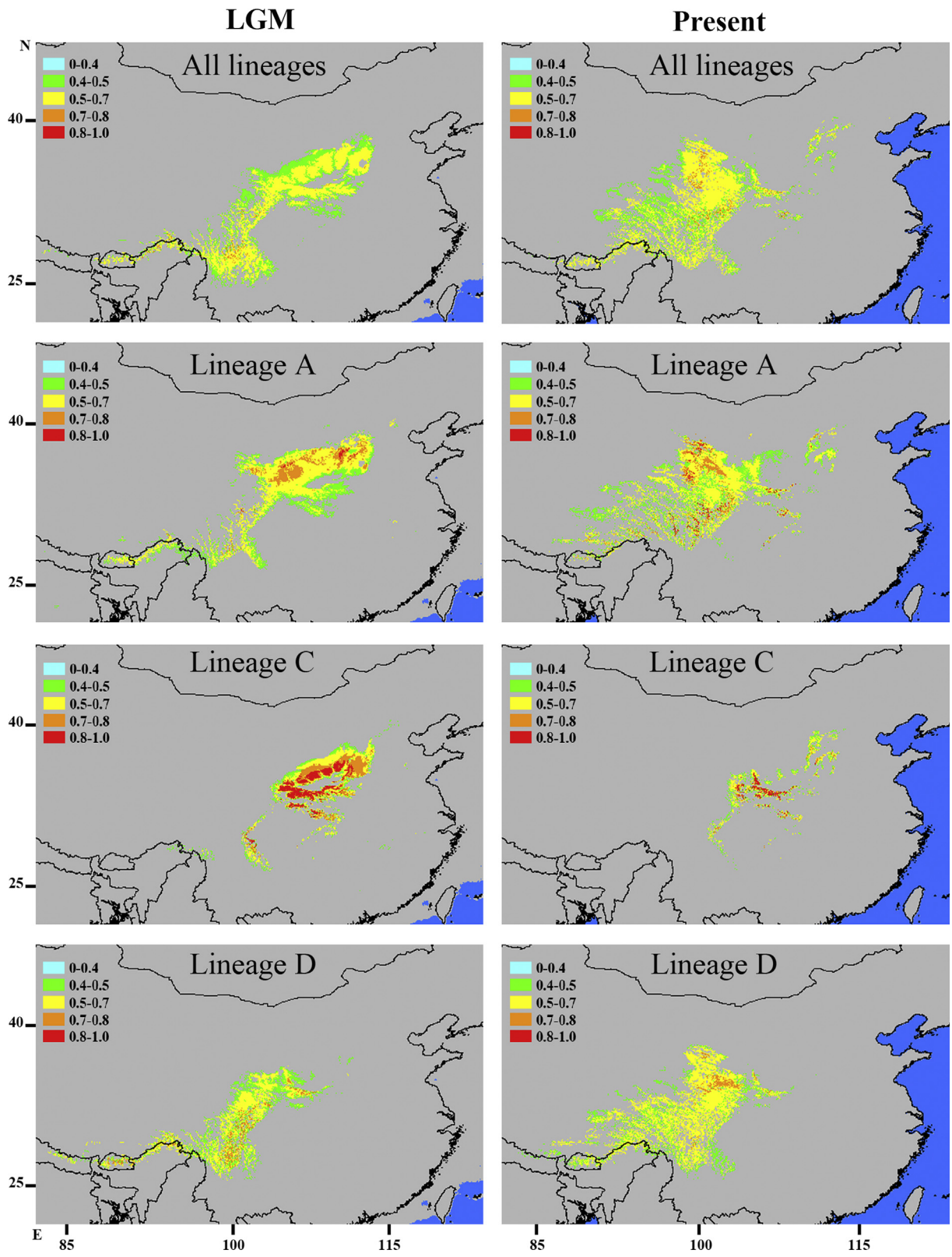

Fig. 6. Potential distribution range of the main lineages within the section *Sikkimensia* in the QTP*sl* and adjacent regions were simulated by Species Distribution Models using bioclimatic variables. Colors represent bioclimatic suitability, from most suitable (red) to unsuitable (gray). LGM: Last Glacial Maximum. (For interpretation of the references to color in this figure legend, the reader is referred to the web version of this article.)

in the QDM of the populations of lineage C, together with the existence of several unsampled haplotypes in the network (Figs. 1, 4 and Table 1), could reflect some extinction in a relatively recent past. Meanwhile, the mismatch analysis dismissed the possibility of expansion event in recent for lineage C (Fig. S2 and Table 4). Fragmentation of a wider population could be an explanation for those results (Chou et al., 2011). These findings would imply that multiple small refuges for forest restricted herb species existed in the QDM and adjacent region, similar to that of

Saruma henryi and *Bupleurum longiradiatum* (Zhou et al., 2010; Zhao et al., 2013).

As a cold-tolerant group, lineage D is distributed in the HMR with a higher average altitude than lineage A (3815 m versus 3015 m) (Table 5). Despite the result of SDM showed that lineage B displayed an obvious range contraction in the HMR during the LGM period, there was a minor range expansion in the western QDM (Fig. 6). The psychrophilic habit and niche conservatism (Wiens and Graham, 2005), together with the QDM possesses warm-humid habitat in comparison to the HMR, supported that the expansion of lineage D from the HMR to the QDM region should be limited. Although the mismatch analysis failed to support that lineage D had undergone expansion event in recent period, we found that the high level of genetic diversity in lineage D had been distributed in multi-area rather than concentrated in a single area (Fig. 1 and Table 1). In addition, the overall cpDNA network is not star-like (Fig. 4a) which also indicated that the expansion model was obviously different from what could be expected from a recent rapid expansion from a single refuge. Previous study suggested that plant species could have survived in high altitude areas during the ice age period (Anderson et al., 2006; Opgenoorth et al., 2010; Allen et al., 2015). Our result indicated that the HMR may have provided multi-refuge model for the cold-tolerant herb species in high altitude area. Similar results have been obtained for other plant taxa in the HMR and adjacent region, such as, *Juniperus tibetica*, *Rhodiola alsia*, *Potentilla glabra* and *Aconitum gymnandrum* (Gao et al., 2009; Wang et al., 2009a, b; Opgenoorth et al., 2010).

5. Conclusion

This study has used the evolutionary history of *Allium* section *Sikkimensia*, along with morphological trait variations and climatic variables, as a model for exploring the effect of the HMR uplifts and Quaternary climatic fluctuations to environment changes in the QTP*sl* and its eastern adjacent area. Molecular dating reveals that the large scale environmental changes following the QTP*sl* uplift during the late Miocene may have triggered the initial split of *Sikkimensia*. Subsequently, environmental and geological effects, involving the intense uplift of the HMR around 3–4 Ma and a putative abrupt intensifying of the Asian monsoon regimes, may drive divergence among lineages (lineage C and D)/within lineage (lineage A) in *Sikkimensia*. In other words, the evolutionary history of the section *Sikkimensia* responds well to the orographic and climatic changes following the HMR uplift. Furthermore, *Sikkimensia* populations exhibited lopsided demographic history in the LGM, as was indicated by the expansion of their range in the QDM and the contraction of distribution range in the HMR. These findings illustrate that the HMR uplift during the late Miocene and the middle Pliocene could have triggered the orographic and environmental changes in the HMR and its eastern adjacent area. Moreover, geological topography also played a crucial role for taxa to respond the climate change that had taken place in the HMR and its eastern adjacent area during the Pleistocene.

Availability of data and materials

The data sets supporting the results of this article are available in the NCBI Genebank, under the accession numbers: MF674579-MF677750 and MH065758-MH067951.

Authors' contributions

XJH and CX designed the study. CX, DFX, XLG and YZ collected the samples. CX, YZ and XLG performed the experiments. CX and DFX performed the analyses. CX, DFX, QL, SDZ and XJH participated in the scientific discussion and commented on the manuscript.

Ethics approval and consent to participate

Not applicable.

Consent for publication

Not applicable.

Competing interests

The author declare that they have no competing interests.

Acknowledgements

This work was financially supported by the National Natural Science Foundation of China (Grant numbers 31872647, 31570198, 31110103911), National Specimen Information Infrastructure, Educational Specimen Sub-Platform (http://mnh.scu.edu.cn/). We are grateful to Prof. Yan Yu, Dr. Min-Jie Li, Dr. Qun-Yin Xiao, Dr. Deng-Feng Xie and Dr. Jiao Huang for their valuable discussions on manuscript, to Heng-Liang Zhang for his help in English grammar, to Jun Wen, Xian-Lin Guo, Yan Zhong, Huan-Xi Yu, Hua-Qiao Yang, Han-Qi Wang and Yong Yan for assistance with collecting samples.

Appendix A. Supplementary material

Supplementary data to this article can be found online at https://doi.org/10.1016/j.ympev.2018.09.011.

References

Allen, G.A., Marr, K.L., McCormick, L.J., Hebda, R.J., 2015. Geographical origins, migration patterns and refugia of Sibbaldia procumbens, an arcticalpine plant with a fragmented range. J. Biogeogr. 42, 1665–1676.
Álvarez, I., Wendel, J.F., 2003. Ribosomal ITS sequences and plant phylogenetic inference. Mol. Phylogenet. Evol. 29, 417–434.
An, Z.S., Kutzbach, J.E., Prell, W.L., Porter, S.C., 2001. Evolution of Asian monsoons and phased uplift of the Himalaya-Tibetan Plateau since Late Miocene times. Nature 411, 62–66.
An, Z.S., Zhang, P.Z., Wang, E., et al., 2006. Changes of the monsoon-arid environment in China and growth of the Tibetan Plateau since the Miocene. Quatern. Sci. 26, 678–693 (in Chinese).
Anderson, E., 1949. Introgressive Hybridization. John Wiley, New York.
Anderson, L.L., Hu, F.S., Nelson, D.M., Petit, R.J., Paige, K.N., 2006. Iceage endurance: DNA evidence of a white spruce refugium in Alaska. Proc. Natl. Acad. Sci. 103, 12447–12450.
Antonelli, A., Nylander, J.A.A., Persson, C., Sanmartin, I., 2009. Tracing the impact of Andean uplift on Neotropical plant evolution. Proc. Natl. Acad. Sci. 106 (24), 9749–9754.
Avise, J.C., 2000. Phylogeography: The History and Formation of Species. Harvard University Press, Cambridge, MA.
Bai, W.N., Liao, W.J., Zhang, D.Y., 2010. Nuclear and chloroplast DNA phylogeography reveal two refuge areas with asymmetrical gene flow in a temperate walnut tree from East Asia. New Phytol. 188, 892–901.
Boos, W.R., Kuang, Z.M., 2010. Dominant control of the South Asian monsoon by orographic insulation versus plateau heating. Nature 463, 218–222.
Boos, W.R., Kuang, Z.M., 2013. Sensitivity of the South Asian monsoon to elevated and non-elevated heating. Sci. Rep. 3, 1192.
Chang, Z., Xiao, J., Lü, L., Yao, H., 2010. Abrupt shifts in the Indian monsoon during the Pliocene marked by high-resolution terrestrial records from the Yuanmou Basin in southwest China. J Asian Earth Sci. 37, 166–175.
Chen, F.B., 1992. H-D event: an important tectonic event of the late Cenozoic in Eastern Asia. Mount. Res. 10, 195–202.
Chen, F.B., 1996. Second discussion on the H-D movement. Mount. Res. 17, 14–22.
Chen, S.C., Kim, D.K., Chase, M.W., Kim, J.H., 2013. Networks in of Asparagales (Lilianae) based on four plastid genes. PLoS ONE 8, e59472.
Chen, S.Y., Wu, G.L., Zhang, D.J., Gao, Q.B., Du, Y.Z., Zhang, F.Q., Chen, S.L., 2008. Potential refugium on the Qinghai-Tibet Plateau revealed by the chloroplast DNA phylogeography of the alpine species Metagentiana striata (Gentianaceae). Biol. J. Linn. Soc. 157, 125–140.
Chou, Y.W., Thomas, P.I., Ge, X.J., LePage, B.A., Wang, C.N., 2011. Refugia phylogeography of Taiwania in East Asia. J. Biogeogr. 38, 1992–2005.
Comes, H.P., Kadereit, J.W., 1998. The effect of Quaternary climatic changes on plant distribution and evolution. Trends Plant Sci. 3, 432–438.
Couper, R.A., 1960. New Zealand Mesozoic and Cainozoic plant microfossils. N. Z. Geol. Surv. Paleontol. Bull. 32, 1–87.

Cun, Y.Z., Wang, X.Q., 2010. Plant recolonization in the Himalaya from the southeastern Qinghai-Tibetan Plateau: geographical isolation contributed to high population differentiation. Mol. Phylogenet. Evol. 56, 972–982.
Davis, M.B., Shaw, R.G., 2001. Range shifts and adaptive responses to Quaternary climate change. Science 292, 673–679.
Degnan, J.H., Rosenberg, N.A., 2009. Gene tree discordance, phylogenetic inference and the multispecies coalescent. Trends Ecol Evol. 24, 332–340.
Ding, L., Spicer, R., Yang, J., et al., 2017. Quantifying the rise of the Himalaya orogen and implications for the South Asian monsoon. Geology 45, 215–218.
Doyle, J.J., Doyle, J.L., 1987. A rapid DNA isolation procedure for small quantities of fresh leaf tissue. Phytochem. Bull. 19, 11–15.
Drummond, A.J., Ho, S.Y.W., Phillips, M.J., Rambaut, A., 2006. Relaxed phylogenetics and dating with confidence. PLoS Biol. 4, 699–710.
Drummond, A.J., Rambaut, A., 2007. BEAST: Bayesian evolutionary analysis by sampling trees. BMC Evol. Biol. 7, 214.
Du, F.K., Peng, X.L., Liu, J.Q., Lascoux, M., Hu, F.S., Petit, R.j., 2011. Direction and extent of organelle DNA introgression between two spruce species in the Qinghai-Tibetan Plateau. New Phytol. 192, 1024–1033.
Du, F.K., Hou, M., Wang, W.T., Mao, K.S., Hampe, A., 2017. Phylogeography of Quercus aquifolioides provides novel insights into the Neogene history of a major global hotspot of plant diversity in south-west China. J. Biogeogr. 44, 294–307.
Elith, J., Leathwick, J.R., 2009. Species distribution models: ecological explanation and prediction across space and time. Annu. Rev. Ecol. Evol. Syst. 40, 677–697.
Excoffier, L., Smouse, P., Quattro, J., 1992. Analysis of molecular variance inferred from metric distances among DNA haplotypes: application to human mitochondrial DNA restriction data. Genetics 131, 479–491.
Excoffier, L., Lischer, H.E., 2010. Arlequin suite version 3.5: a new series of programs to perform population genetics analyses under Linux and Windows. Mol. Ecol. Resour. 10, 564–567.
Favre, A., Päckert, M., Pauls, S.U., Jähnig, S.C., Uhl, D., Michalak, I., et al., 2015. The role of the uplift of the Qinghai-Tibetan plateau for the evolution of Tibetan biotas. Biol. Rev. 90, 236–253.
Fielding, A.H., Bell, J.F., 1997. A review of methods for the assessment of prediction errors in conservation presence/absence models. Environ. Conserv. 24, 38–49.
Fritsch, R.M., 2001. Taxonomy of the genus *Allium* – contributions from IPK Gatersleben. Herbertia 56, 19–50.
Fritsch, R.M., Friesen, N., 2002. Evolution, domestication, and taxonomy. In: Rabinowitch, H.D., Currah, L. (Eds.), Allium Crop Science: Recent Advances. CABI Publishing, Wallingford, UK, pp. 5–30.
Friesen, N., Fritsch, R.M., Pollner, S., Blattner, F.R., 2000. Molecular and morphological evidence for an origin of the aberrant genus Milula within Himalayan species of *Allium* (Alliaceae). Mol. Phylogenet. Evol. 17, 209–218.
Friesen, N., Fritsch, R.M., Blattner, F.R., 2006. Phylogeny and new intrageneric classification of *Allium* (Alliaceae) based on nuclear ribosomal DNA ITS sequences. Aliso 22, 372–395.
Gao, Q.B., Zhang, D.J., Chen, S.Y., Duan, Y.Z., Zhang, F.Q., Li, Y.H., Chen, S.L., 2009. Chloroplast DNA phylogeography of *Rhodiola alsia* (Crassulaceae) in the Qinghai-Tibet Plateau. Botany 87, 1077–1088.
Gao, Q.B., Zhang, D.J., Duan, Y.Z., Zhang, F.Q., Li, Y.H., Fu, P.C., Chen, S.L., 2012. Intraspecific divergences of *Rhodiola alsia* (Crassulaceae) based on plastid DNA and internal transcribed spacer fragments. Bot. J. Linn. Soc. 168, 204–215.
George, A.D., Marshallsea, S.J., Wyrwoll, K.H., Chen, J., Lu, Y.C., 2001. Miocene cooling in the northern Qilian Shan, northeasternmargin of the Tibetan Plateau, revealed by apatite fission-track and vitrinite-reflectance analysis. Geology 29, 939–942.
Goslee, S.C., Urban, D.L., 2007. The ecodist package for dissimilarity-based analysis of ecological data. J. Stat. Softw. 22, 1–19.
Guo, Z.T., Ruddiman, W.F., Hao, Q.Z., et al., 2002. Onset of Asian desertification by 22 Myr ago inferred from loess deposits in China. Nature 416, 159–163.
Harpending, H.C., 1994. Signature of ancient population growth in a lowresolution mitochondrial DNA mismatch distribution. Hum. Biol. 66, 591–600.
Harrison, T.M., Copeland, P., Kidd, W.S.F., Yin, A., 1992. Raising Tibet. Science 255, 1663–1670.
Herendeen, P.S., Crane, P.R., 1995. The fossil history of the monocotyledons. In: Rudall, P.J., Cribb, P.J., Cutler, D.F., Humphries, C.J. (Eds.), Monocotyledons: Systematics and Evolution. Kew: Royal Botanic Gardens, 570.
Hewitt, G.M., 1996. Some genetic consequences of ice ages, and their role in divergence and speciation. Biol. J. Linn. Soc. 58, 247–276.
Hewitt, G.M., 1999. Post-glacial re-colonization of European biota. Biol. J. Linn. Soc. 68, 87–112.
Hewitt, G.M., 2004. Genetic consequences of climatic oscillations in the Quaternary. Philos. Trans. Roy. Soc. B 359, 183–195.
Hickerson, M.J., Carstens, B.C., Cavender-Bares, J., Crandall, K.A., Graham, C.H., Johnson, J.B., et al., 2010. Phylogeography's past, present, and future: 10 years after. Mol. Phylogenet. Evol. 54, 291–301.
Hijmans, R.J., Guarino, L., Cruz, M., Rojas, E., 2001. Computer tools for spatial analysis of plant genetic resources data: 1. DIVA-GIS. PGR Newslett. 127, 15–19.
Hijmans, R.J., Cameron, S.E., Parra, J.L., Jones, P.G., Jarvis, A., 2005. Very high resolution interpolated climate surfaces for global land areas. Int. J. Climatol. 25, 1965–1978.
Janssen, T., Bremer, K., 2004. The age of major monocot groups inferred from 800+*rbcL* sequences. Bot. J. Linn. Soc. 146, 385–398.
Jia, D.R., Liu, T.L., Wang, L.Y., Zhou, D.W., Liu, J.Q., 2011. Evolutionary history of an alpine shrub *Hippophaé tibetana* (Elaeagnaceae): allopatric divergence and regional expansion. Biol. J. Linn. Soc. 102, 37–50.
Kou, X.Y., Ferguson, D.K., Xu, J.X., Wang, Y.F., Li, C.S., 2006. The reconstruction of paleovegetation and paleoclimate in the Late Pliocene of West Yunnan. China Clim. Change 77, 431–448.
Larkin, M.A., Blackshields, G., Brown, N.P., et al., 2007. Clustal W and Clustal X version 2.0. Bioinformatics 23, 2947–2948.
Librado, P., Rozas, J., 2009. DnaSP version 5: a software for comprehensive analysis of DNA polymorphism data. Bioinformatics 25, 1451–1452.
Li, J.J., Fang, X.M., 1999. Uplift of the Tibetan Plateau and environmental changes. Chin. Sci. Bull. 44, 2117–2124.
Li, L., Abbott, R.J., Liu, B., Sun, Y., Li, L., Zou, J.B., et al., 2013. Pliocene intraspecific divergence and Plio-Pleistocene range expansions within *Picea likiangensis* (Lijiang spruce), a dominant forest tree of the Qinghai-Tibet Plateau. Mol. Ecol. 22, 5237–5255.
Li, M.J., Tan, J.B., Xie, D.F., Huang, D.Q., Gao, Y.D., He, X.J., 2016. Revisiting the evolutionary events in *Allium* subgenus *Cyathophora* (Amaryllidaceae): insights into the effect of the Hengduan Mountains Region (HMR) uplift and Quaternary climatic fluctuations to the environmental changes in the Qinghai-Tibet Plateau. Mol. Phylogenet. Evol. 94, 802–813.
Li, Q.Q., Zhou, S.D., He, X.J., Yu, Y., Zhang, Y.C., Wei, X.Q., 2010. Phylogeny and biogeography of *Allium* (Amaryllidaceae: Allieae) based on nuclear ribosomal internal transcribed spacer and chloroplast rps16 sequences, focusing on the inclusion of species endemic to China. Ann. Bot. 106, 709–733.
Liang, Q.L., Xu, X.T., Mao, K.S., Wang, M.C., Wang, K., Xi, Z.X., Liu, J.Q., 2018. Shift in plant distributions in response to climate warming in a biodiversity hotspot, the Hengduan Mountains. J. Biogeogr. https://doi.org/10.1111/jbi.13229.
Lippert, P.C., van Hinsbergen, D.J.J., Dupont-Nivet, G., 2014. Early Cretaceous to present latitude of the central proto- Tibetan Plateau: a paleomagnetic synthesis with implications for Cenozoic tectonics, paleogeography, and climate of Asia. In: Nie, J., Horton, B.K., Hoke, G.D. (Eds.), Toward an Improved Understanding of Uplift Mechanisms and the Elevation History of the Tibetan Plateau. Geological Society of America Special Paper, 507, pp. 1–21.
Liu, J., Michael, M., Jim, P., Gao, L.M., Ram, C.P., Li, D.Z., 2013. Geological and ecological factors drive cryptic speciation of yews in a biodiversity hotspot. New Phytol. 199, 1093–1108.
Liu, J.Q., Sun, Y.S., Ge, X.J., Gao, L.M., Qiu, Y.X., 2012. Phylogeographic studies of plant in China: advances in the past and directions in the future. J. Syst. Evol. 50, 267–275.
Liu, J.Q., Duan, Y.W., Hao, G., Ge, X.J., Sun, H., 2014. Evolutionary history and underlying adaptation of alpine plants on the Qinghai-Tibet Plateau. J. Syst. Evol. 52, 241–249.
Liu, X.D., Dong, B.W., 2013. Influence of the Tibetan Plateau uplift on the Asian monsoon-arid environment evolution. Geology 58, 4277–4291.
Luo, D., Yue, J.P., Sun, W.G., et al., 2016. Evolutionary history of the subnival flora of the Himalaya-Hengduan Mountains: first insights from comparative phylogeography of four perennial herbs. J. Biogeogr. 43, 31–43.
Manly, B.F.J., 1997. Randomization, Bootstrap and Monte Carlo Methods in Biology, second ed. Chapman & Hall, London.
Marchese, C., 2015. Biodiversity hotspots: a shortcut for a more complicated concept. Glob. Ecol. Conserv. 3, 297–309.
McGuire, J.A., Linkem, C.W., Koo, M.S., et al., 2007. Mitochondrial introgression and incomplete lineage sorting through space and time: phylogenetics of *crotaphytid lizards*. Evolution 6, 2879–2897.
Meng, H.H., Tao, S., Gao, X.Y., Li, J., Jiang, X.L., Sun, H., Zhou, Z.K., 2017. Warm-cold colonization: response pf oaks to uplift of the Himalaya-Hengduan Mountains. Mol. Ecol. 26, 3276–3294.
Miller, M.A., Pfeiffer, W., Schwartz, T., 2010. Creating the CIPRES Science Gateway for inference of large phylogenetic trees. In: Proceedings of the Gateway Computing Environments Workshop (GCE), New Orleans, LA, pp. 1–8.
Moore, W.S., 1995. Inferring phylogenies from mtDNA variation: Mitochondrial-gene trees versus nuclear-gene trees. Evolution 49, 718–726.
Mulch, A., Chamberlain, C.P., 2006. Earth science: the rise and growth of Tibet. Nature 439, 670–671.
Muller, J., 1981. Fossil pollen of extant angiosperms. Bot. Rev. 47, 1–142.
Myers, N., Mittermeier, R.A., Mittermeier, C.G., Da, F.G., Kent, J., 2000. Biodiversity hotspots for conservation priorities. Nature 403, 853–858.
Nylander, J.A.A., 2004. MrModelTest 2.2: Program Distributed by the Author. Evolutionary Biology. University Centre, Uppsala < http://www.abc.se/~nylander/ > .
Opgenoorth, L., Vendramin, G.G., Mao, K., Miehe, G., Miehe, S., Liepelt, S., et al., 2010. Tree endurance on the Tibetan Plateau marks the world's highest known tree line of the Last Glacial Maximum. New Phytol. 185, 332–342.
Peterson, A.T., Papes, M., Soberon, J., 2008. Rethinking receiver operating characteristic analysis applications in ecological niche modeling. Ecol. Model. 213, 63–72.
Phillips, S.J., Anderson, R.P., Schapire, R.E., 2006. Maximum entropy modeling of species geographic distributions. Ecol. Model. 190, 231–259.
Polzin, T., Daneshmand, S.V., 2003. On Steiner trees and minimum spanning trees in hypergraphs. Oper. Res. Lett. 31, 12–20.
Pons, O., Petit, R.J., 1996. Measuring and testing genetic differentiation with ordered versus unordered alleles. Genetics 144, 1237–1245.
Qian, H., Ricklefs, R.E., 2000. Large-scale processes and the Asian bias in species diversity of temperate plants. Nature 407, 180–182.
Qiu, Y.X., Fu, C.X., Comes, H.P., 2011. Plant molecular phylogeography in China and adjacent regions, tracing the genetic imprints of Quaternary climate and environmental change in the world's most diverse temperate flora. Mol. Phylogenet. Evol. 59, 225–244.
Qu, Y.H., Ericson, P.G., Quan, Q., Song, G., Zhang, R.Y., Gao, B., 2014. Long-term isolation and stability explain high genetic diversity in the Eastern Himalaya. Mol. Ecol. 23, 705–720.
Raamsdonk, L.W.V., Smiech, M.P., Sandbrink, J.M., 1997. Introgression explains

incongruence between nuclear and chloroplast DNA-based phylogenies in *Allium* Section *Cepa*. Bot. J. Linn. Soc. 123, 91–108.
Rautenberg, A., Hathaway, L., Oxelman, B., Prentice, H.C., 2010. Geographic and phylogenetic patterns in *Silene* section *Melandrium* (Caryophyllaceae) as inferred from chloroplast and nuclear DNA sequences. Mol. Phylogenet. Evol. 57, 978–991.
Renner, S.S., 2016. Available data point to a 4-km-high Tibetan Plateau by 40 Ma, but 100 molecular-clock papers have linked supposed recent uplift to young node ages. J. Biogeogr. 43, 1479–1487.
Ronquist, F., Teslenko, M., van der Mark, P., Ayres, D.L., Darling, A., Hohna, S., Larget, B., Liu, L., Suchard, M.A., Huelsenbeck, J.P., 2012. Mr Bayes 3.2: efficient Bayesian phylogenetic inference and model choice across a large model space. Syst. Biol. 61, 539–542.
Rowley, D.B., Currie, B.S., 2006. Palaeo–altimetry of the late Eocene to Miocene Lunpola basin, central Tibet. Nature 439, 677–681.
Royden, L.H., Burchfiel, B.C., van der Hils, T.R.D., 2008. The geological evolution of the Tibetan plateau. Science 321, 1054–1058.
Shaw, J., Lickey, E.B., Beck, J.T., Farmer, S.B., Liu, W.S., Miller, J., Siripun, K.C., Winder, C.T., Schilling, E.E., Small, R.L., 2005. The tortoise and the hare II: relative utility of 21 noncoding chloroplast DNA sequences for phylogenetic analysis. Am. J. Bot. 92, 142–166.
Shaw, J., Lickey, E., Schilling, E., Small, R., 2007. Comparison of whole chloroplast genome sequences to choose noncoding regions for phylogenetic studies in angiosperms: the tortoise and the hare III. Am. J. Bot. 94, 275–288.
Shahzad, K., Jia, Y., Chen, F.L., Zeb, U., Li, Z.H., 2017. Effects of mountain uplift and climatic oscillations on phylogeography and species divergence in four endangered *Notopterygium* Herbs. Front. Plant Sci. 8, 1929.
Shi, Y.F., Zheng, B.X., Li, S.J., Ye, B.S., 1995. Studies on altitude and climatic environment in the middle and east parts of Tibetan Plateau during Quaternary Maximum Glaciation. J. Glaciol. Geocryol. 17, 97–112.
Shi, Y.F., Li, J.J., Li, B.Y., 1998. Uplift and Environmental Changes of Qinghai-Tibetan Plateau in the Late Cenozoic. Guangdong Science and Technology Press, Guangzhou, China.
Smouse, P.E., Long, J.C., Sokal, R.R., 1986. Multiple regression and correlation extensions of the Mantel test of matrix correspondence. Systemat. Zool. 35, 627–632.
Sun, B.N., Wu, J.Y., Liu, Y.S.C., Ding, S.T., Li, X.C., Xie, S.P., Yan, D.F., Lin, Z.C., 2011. Reconstructing Neogene vegetation and climates to infer tectonic uplift in western Yunnan, China. Palaeogeogr. Palaeoclimatol. Palaeoecol. 304, 328–336.
Swofford, D.L., 2003. PAUP/ Version 4.0b10: Phylogenetic Analysis using Parsimony/and Other Methods. Sinauer Associates, Sunderland.
Taberlet, P., Fumagalli, L., Wust-Saucy, A.G., Cosson, J.F., 1998. Comparative phylogeography and postglacial colonization routes in Europe. Mol. Ecol. 7, 453–464.
Tank, D.C., Eastman, J.M., Pennell, W.M., Soltis, P.S., Soltis, D.E., Hinchliff, C.E., Brown, J.W., Sessa, E.B., Harmon, L.J., 2015. Nested radiations and the pulse of angiosperm diversification: increased diversification rates often follow whole genome duplications. New Phytol. 207, 454–467.
Tian, B., Liu, R.R., Wang, L.Y., Qiu, Q., Chen, K.M., Liu, J.Q., 2009. Phylogeographic analyses suggest that a deciduous species (*Ostryopsis davidiana* Decne., Betulaceae) survived in northern China during the Last Glacial Maximum. J. Biogeogr. 36, 2148–2155.
Wan, S., Li, A.C., Clift, P.D., Stuut, J.B.W., 2007. Development of the East Asian monsoon: mineralogical and sedimentological records in the northern South China Sea since 20 Ma. Palaeogeogr. Palaeoclimatol. Palaeoecol. 254, 561–582.
Wang, L.Y., Abbott, R.J., Zheng, W., Chen, P., Wang, Y.J., Liu, J.Q., 2009a. History and evolution of alpine plants endemic to the Qinghai-Tibetan Plateau: *Aconitum gymnandrum* (Ranunculaceae). Mol. Ecol. 18, 709–721.
Wang, L.Y., Ikeda, H., Liu, T.L., Wang, Y.J., Liu, J.Q., 2009b. Repeated range expansion and glacial endurance of *Potentilla glabra* (Rosaceae) in the Qinghai-Tibetan Plateau. J Integr Plant Biol. 51, 698–706.
Wang, Z., Du, S., Dayanandan, S., Wang, D., Zeng, Y., Zhang, J., 2014. Phylogeny reconstruction and hybrid analysis of *Populus* (Salicaceae) based on nucleotide sequences of multiple single-copy nuclear genes and plastid fragments. PLoS ONE. 9, e103645.
Wen, J., Zhang, J.Q., Nie, Z.L., Zhong, Y., Sun, H., 2014. Evolutionary diversifications of plants on the Qinghai-Tibetan Plateau. Front. Genet. 5, 1–16.
White, T.J., Bruns, T., Lee, S., Taylor, J., 1990. Amplification and direct sequencing of fungal ribosomal RNA genes for phylogenetics. In: Innis, M.A., Gelfand, D.H., Shinsky, J.J., White, T.J. (Eds.), PCR Protocols: A Guide to Methods and Applications. Academic Press, San Diego, pp. 315–322.
Wiens, J.J., Graham, C.H., 2005. NICHE CONSERVATISM: interrating evolution, ecology, and conservation biology. Annu. Rev. Ecol. Evol. Syst. 36, 519–539.
Wikström, N., Savolainen, V., Chase, M.W., 2001. Evolution of the angiosperms: calibrating the family tree. Philos. Trans. R. Soc. 268, 2211–2220.
Wolfe, K.H., Li, W.H., Sharp, P.M., 1987. Rates of nucleotide substitution vary greatly among plant mitochondrial, chloroplast, and nuclear DNAs. Proc. Natl. Acad. Sci. 84, 9054–9058.
Wright, S.D., Yong, C.G., Wichman, S.R., Dawson, J.W., Gardner, R.C., 2001. Stepping stones to Hawaii: a trans-equatorial dispersal pathway for Metrosideros (Myrtaceae) inferred from nrDNA (ITS + ETS). J. Biogeogr. 28, 769–774.
Wu, Y.Q., Cui, Z.J., Liu, G.N., Ge, D.K., Yin, J.R., Xu, Q.H., Pang, Q.Q., 2001. Quaternary geomorphological evolution of the Kunlun Pass area and uplift of the Qinghai-Xizang (Tibet) Plateau. Geomorphology 36, 203–216.
Wu, Z.Y., 1979. The regionalization of Chinese flora. Res. Yunnan Plant 1, 21–22.
Wu, Z.Y., Wu, S.G., 1996. A proposal for a new floristic kingdom (realm)-the E. Asiatic kingdom, its delineation and characteristics. In: Zhang, A.L., Wu, S.G. (Eds.), Floristic Characteristics and Diversity of East Asian Plants. China Higher Education Press, Beijing, pp. 3–42.
Xing, Y., Ree, R.H., 2017. Uplift-driven diversification in the Hengduan Mountains, a temperate biodiversity hotspot. Proc. Natl. Acad. Sci. 114, E3444–E3451.
Xu, T.T., Abbott, R.J., Milne, R.I., Mao, K., Du, F.K., Wu, G.L., Ciren, Z.X., Miehe, G., Liu, J.Q., 2010. Phylogeography and allopatric divergence of cypress species (*Cupressus* L.) in the Qinghai-Tibetan Plateau and adjacent regions. BMC Evol. Biol. 10, 194.
Yang, F.S., Li, Y.F., Ding, X., Wang, X.Q., 2008. Extensive population expansion of *Pedicularis longiflora* (Orobanchaceae) on the Qinghai-Tibetan Plateau and its correlation with the Quaternary climate change. Mol. Ecol. 17, 5135–5145.
Yang, F.S., Qin, A.L., Li, Y.F., Wang, X.Q., 2012. Great genetic differentiation among populations of *Meconopsis integrifolia* and its implication for plant speciation in the Qinghai-Tibetan Plateau. PLoS ONE 7, e37196.
Yamane, K., Yano, K., Kawahara, T., 2006. Pattern and rate of indel evolution inferred from whole chloroplast intergenic regions in sugarcane, maize and rice. DNA Res. 13, 197–204.
Yao, Y.F., Bruch, A.A., Cheng, Y.M., Mosbrugger, V., Wang, Y.F., Li, C.S., 2012. Monsoon vs uplift in Southwestern China-Late Pliocene climate in Yuanmou basin, Yunnan. PLoS ONE 7, e37760.
Yin, A., Harrison, T.M., 2000. Geologic evolution of the Himalayan- Tibetan orogen. Annu. Rev. Earth Planet. Sci. 28, 211–280.
Young, N., Carter, L., Evangelista, P., 2011. A MaxEnt Model version 3. 3.3e Tutorial (Arc GIS version 10). Natural Resource Ecology Laboratory at Colorado State University and the National Institute of Invasive Species Science, Colorado.
Yu, Y., Harris, A.J., Blair, C., He, X.J., 2015. RASP (Reconstruct Ancestral State in Phylogenies): a tool for historical biogeography. Mol. Phylogenet. Evol. 87, 46–49.
Yuan, Q.J., Zhang, Z.Y., Peng, H., Ge, S., 2008. Chloroplast phylogeography of *Dipentodon* (Dipentodontaceae) in southwest China and northern Vietnam. Mol. Ecol. 17, 1054–1065.
Zanne, A.E., Tank, D.C., Cornwell, W.K., Eastman, J.M., et al., 2014. Three keys to the radiation of angiosperms into freezing environments. Nature 506, 89–92.
Zhang, Q., Chiang, T.Y., George, M., Liu, J.Q., Abbott, R.J., 2005. Phylogeography of the Qinghai-Tibetan Plateau endemic *Juniperus przewalskii* (Cupressaceae) inferred from chloroplast DNA sequence variation. Mol. Ecol. 14, 3513–3524.
Zhang, Q.Q., Ferguson, D.K., Mosbrugger, V., Wang, Y.F., Li, C.S., 2012. Vegetation and climatic changes of SW China in response to the uplift of Tibetan Plateau. Palaeogeogr. Palaeoclimatol. Palaeoecol. 363, 23–36.
Zhang, Y.L., Li, B.L., Zheng, D., 2002. A discussion on the boundary and area of the Tibetan Plateau in China. Geogr. Res. 21, 1–8.
Zhao, C., Wang, C.B., Ma, X.G., Liang, Q.L., He, X.J., 2013. Phylogeographic analysis of a temperate-deciduous forest restricted plant (*Bupleurum longiradiatum* Turcz.) reveals two refuge areas in China with subsequent refugial isolation promoting speciation. Mol. Phylogenet. Evol. 68, 628–643.
Zhao, J.L., Xia, Y.M., Cannon, C.H., Kress, W.J., Li, Q.J., 2015. Evolutionary diversification of alpine ginger reflects the early uplift of the Himalayan-Tibetan Plateau and rapid extrusion of Indochina. Gondwana Res. 32, 232–241.
Zheng, D., 1996. The system of physico-geographical regions of the Qinghai-Tibet (Xizang) Plateau. Sci. China (Series D) 39, 410–417.
Zhou, T.H., Li, S., Qian, Z.Q., Su, H.L., Huang, Z.H., Guo, Z.G., Dai, P.F., Liu, Z.L., Zhao, G.F., 2010. Strong phylogeographic pattern of cpDNA variation reveals multiple glacial refugia for *Saruma henryi* Oliv. (Aristolochiaceae), an endangered herb endemic to China. Mol. Phylogenet. Evol. 57, 176–188.